Wegener Center for Climate and Global Change
University of Graz
Atmospheric Remote Sensing and Climate System Research Group
ARSCliSys - on the art of understanding the climate system

WegCenter/UniGraz Technical Report for ESA/ESTEC No. 1/2006

Project:

Prodex-CN1 — Advanced Topics in RO Modelling and Retrieval
[ESA Prodex Arrangement No. 90152-CN1]

Advanced Wave-Optics Forward Modeling and Bending Angle and Transmission Retrieval including Turbulent Random Refractivity Field Modeling

by

Michael E. Gorbunov[1,2], Gottfried Kirchengast[2], and Kent B. Lauritsen[3]

[1] Institute of Atmospheric Physics, Moscow, Russia
[2] Wegener Center and IGAM/Inst. of Physics, University of Graz, Graz, Austria
[3] Danish Meteorological Institute, Copenhagen, Denmark

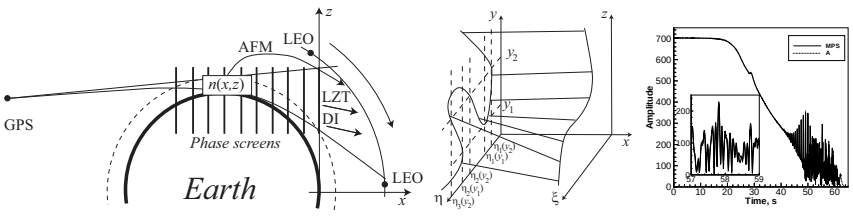

July 2006

Advanced wave-optics forward modeling and bending angle and transmission retrieval including turbulent random refractivity field modeling

M. E. Gorbunov[1,2], G. Kirchengast[2], and K. B. Lauritsen[3]

[1] Institute of Atmospheric Physics, Moscow, Russia

[2] Wegener Center and IGAM/Inst. of Physics, University of Graz, Graz, Austria

[3] Danish Meteorological Institute, Copenhagen, Denmark

Abstract

Fourier Integral Operators (FIOs) are used for constructing asymptotic solutions of wave problems and for the generalization of the geometrical optics. Geometric optical rays are described by the canonical Hamilton system, which can be written in different canonical coordinates in the phase space. The theory of FIOs generalizes the formalism of canonical transforms for solving wave problems. The FIO associated with a canonical transform maps the wave field to a different representation. Mapping to the representation of ray impact parameter was used in the formulation of the Canonical Transform (CT) method for processing radio occultation data. The Full-Spectrum Inversion (FSI) method can also be looked at as an FIO associated with a canonical transform of a different type.

We discuss the general principles of the theory of FIOs and formulate a generalization of the CT and FSI techniques. We derive the FIO that maps radio occultation data measured along the LEO orbit without first applying back propagation. This operator is used for the retrieval of refraction angles and atmospheric absorption. We give a closed derivation of the exact phase function of the FIO obtained in the 'phase matching' approach by Jensen et al. We derive a novel FIO algorithm denoted CT2, which is a modification and improvement of FSI. We discuss the use of FIOs for asymptotic direct modeling of radio occultation data. This direct model is numerically much faster then the multiple phase screen technique. This is especially useful for simulating LEO-LEO occultations at frequencies 10-30 GHz.

The multiple phase screens technique is often used for modeling wave propagation and radio occultation sounding of the atmosphere. The last step of this procedure is the propagation from the last phase screen to the observation orbit of the space-borne receiver. This step was formerly performed by the computation of multiple diffractive integrals, which impairs the numerical efficiency of the algorithm. We introduce an asymptotic method of wave propagation in vacuum from

the last phase screen to a generic observation path. The exact solution is written in the form of the Zverev Transform, which belongs to the class of Fourier Integral Operators (FIO). The phase function of such an operator can be derived from the geometric optical equations. We construct an approximation for the Zverev Transform, utilizing the linearization of the equation of the geometric optical ray propagation in the vicinity of a smooth model of the ray structure. This reduces the corresponding operator to the composition of nonlinear coordinate transforms, multiplication with reference signals, and a Fourier transform. This allows for the design of a fast numerical algorithm based on an FFT.

Numerical simulations are performed based on realistic gridded global fields of meteorological parameters. The new method based on the Linearized Zverev Transform is compared with the standard combination of multiple phase screens and diffractive integrals and with the asymptotic forward modelling for the propagation of centimeter waves in the atmosphere on limb paths. The simulations demonstrate a high accuracy and numerical efficiency of the proposed method.

For modeling wave propagation in a turbulent atmosphere we developed a turbulence model based on the theoretical and experimental studies. We adopt an anisotropic turbulence model with a power spectrum with the exponent that equal -4 for the 2D model (equivalent to -5 for 3D model). The internal scale equals 15 m, and the external scale is 100 m. We use constant anisotropy that takes values from 3 to 50. For numerical simulation we generated realizations of random field with given power spectrum.

Contents

1 Analysis of wave fields by Fourier Integral Operators and their application for radio occultations **5**
1.1 Introduction 5
1.2 Asymptotic Solutions of Wave Problems 7
1.2.1 Maslov Operator 7
1.2.2 Fourier Integral Operators 10
1.2.3 Canonical Transforms 13
1.3 Processing Radio Occultations 14
1.3.1 Canonical Transform without Back Propagation 14
1.3.2 Phase Function 15
1.3.3 Amplitude Function 17
1.3.4 Representation of Approximate Impact Parameter . . . 19
1.4 Direct Modeling 21
1.5 Numerical Simulations 22

2 Conclusions on utility of Fourier Integral Operators for RO **25**

3 Asymptotic methods of modeling the propagation of centimeter waves in the atmosphere on limb paths **27**
3.1 Introduction 27
3.2 Fourier Integral Operator Solution for Wave Propagation from the Last Phase Screen to the Observation Orbit 28
3.3 Numerical Simulations 34
3.4 Conclusions 36

4 Turbulent random refractivity field modeling **39**

5 References **43**

6 Figures **49**

1 Analysis of wave fields by Fourier Integral Operators and their application for radio occultations

1.1 Introduction

In this paper we discuss the application of Fourier Integral Operators (FIOs) for processing radio occultation data. The FIO is a technique for constructing short-wave asymptotic solutions of wave problems. The simplest short-wave asymptotic solution is geometric optics (GO) (*Kravtsov and Orlov*, 1990). It has the following limitations of the applicability: (1) It cannot describe details of wave fields with small characteristic scales below the Fresnel zone size, (2) it does not work on caustics, where the GO amplitude goes to infinity. A generalization of asymptotic GO solution for quantum mechanics and theory of waves in inhomogeneous media was introduced in two equivalent forms: (1) the technique of Maslov operators and (2) FIO (*Maslov and Fedoriuk*, 1981; *Mishchenko et al.*, 1990; *Hörmander*, 1985a,b). This technique significantly reduces the limitation due to Fresnel diffraction. In particular, the FIO asymptotic solution in a vacuum coincides with the exact solution.

Processing radio occultation data posed the inverse problem: reconstruction of the GO rays from measurements of wave fields, especially in multipath zones. The simplest GO approximation, which can only be applied in single-ray areas, uses the connection between ray direction and Doppler frequency (*Vorob'ev and Krasil'nikova*, 1994). The resolution of this approximation is limited by the Fresnel zone. Analysis of local spatial spectra is a simple technique that can separate multiple rays. It was applied for processing planetary occultations (*Lindal et al.*, 1987), and it was also used for the analysis of GPS radio occultation data for the Earth's atmosphere, obtained by Microlab-1 and CHAMP satellites (*Pavelyev*, 1998; *Igarashi et al.*, 2000; *Pavelyev et al.*, 2002; *Gorbunov*, 2002b, e.g.). Another direction took origin from the early work by *Marouf et al.* (1986), who suggested the back propagation (BP) technique for the reconstruction of Saturn rings. This technique reduced the effects of diffraction at a large propagation distance. A very similar Fresnel inversion, based on the thin screen approximation, was introduced by *Melbourne et al.* (1994) and applied by *Mortensen and Høeg* (1998). And the combination of BP preprocessing with the standard GO inversion, which does not use the thin screen model, was suggested by *Gorbunov and Gurvich* (1998a,b).

The application of Fourier Integral Operators for processing radio occultations was suggested by *Gorbunov* (2002a,b) in the framework of the

Canonical Transform (CT) method. The CT method uses back propagation as the preprocessing tool, which reduces the radio occultation geometry to a vertical observation line. The CT method uses the phase space with coordinate y along the vertical line and conjugated momentum η (vertical projection of ray direction vector). In single-ray areas the momentum is equal to the derivative of the eikonal (optical path) of the wave field. The back-propagated complex wave field u as a function of vertical coordinate y is subjected to the Fourier Integral Operator associated with a canonical transform from (y, η) to (p, ξ), where p is the ray impact parameter, and the momentum, ξ, conjugated with it is equal to the ray direction angle. Under the assumption that each value of the impact parameter occurs not more than once, this transform allows for disentangling multiple rays. The phase of the transformed wave field can then be differentiated with respect to the impact parameter p giving the ray direction angle ξ, which is linked to refraction (bending) angle by simple geometrical relationships. The CT method provides high accuracy and resolution in the reconstruction of refraction angle profiles. The FIO used in its formulation allows for a fast numerical implementation on the basis of FFT. The disadvantage of this CT method is the necessity of BP, which is the most time-consuming part of the numerical algorithm. However, a very fast implementation of BP can be designed using a simple geometric optical approximation (S. Sokolovskiy, private communication). Also, the best implementations of BP using numerical computation of diffractive integral are reasonably fast.

The Full Spectrum Inversion (FSI) method was recently introduced by *Jensen et al.* (2003). The simplest formulation of this method applies to a radio occultation with a circular geometry (i.e., spherical satellite orbits in the same vertical plane, spherical Earth and spherically symmetrical atmosphere). The Fourier transform is applied to the complete record of the complex field $u(t)$ as function of observation time t or another parameterization of the observation trajectory such as satellite-to-satellite angle. For circular occultation geometry, the derivative of the phase, or the Doppler frequency ω, of the wave field $u(t)$ is proportional to ray impact parameter p. We can introduce the (multi-valued) dependence $\omega(t)$, which is by definition equal to Doppler frequency (or frequencies) of the ray(s) received at time moment t. In multi-path zones, where the dependence $\omega(t)$ is multi-valued, it cannot be found by the differentiation of the phase of the wave field $u(t)$. Unlike $\omega(t)$, the inverse dependence $t(\omega)$ is single-valued, if we assume that each impact parameter and therefore frequency ω occurs not more than once. Using a stationary phase derivation, it can be easily shown that the derivative of the phase of the Fourier spectrum $\tilde{u}(\omega)$ equals $-t(\omega)$. Then, for each impact parameter p we can find the time t and therefore the positions of the

GPS satellite and low-Earth orbiter (LEO) for which this impact parameter occurred. This allows for the computation of the corresponding refraction angle. The advantage of this method is its numerical simplicity. Its disadvantage is that it is formulated for circular radio occultation geometry and its generalization for realistic radio occultations required some approximation.

Gorbunov and Lauritsen (2002) suggested a synthesis of the CT and FSI methods. They derived a general formula for the FIO applied directly to radio occultation data measured along a generic LEO trajectory without the BP procedure. The phase function of the FIO is described by a differential equation. The equation was approximately solved for a generic occultation geometry, to first order in a small parameter measuring the deviation from a circular orbit. It was shown that for a circular occultation geometry this operator reduces to a Fourier transform. This method was thus a generalization of the FSI technique for generic observation geometry. Recently, *Jensen et al.* (2004) obtained the exact expression for the phase function of the FIO introduced by *Gorbunov and Lauritsen* (2002). *Jensen et al.* (2004) also considered the amplitude function and below we shall use the synthesis of the approaches used by *Jensen et al.* (2004) and by *Gorbunov* (2002a,b).

1.2 Asymptotic Solutions of Wave Problems

1.2.1 Maslov Operator

The technique of Maslov operators was developed for solving the Schrödinger equation in quantum mechanics and pseudo-differential or parabolic equation in the theory of waves in inhomogeneous medium. In quantum mechanics, a particle with momentum $\mathbf{p}$ and energy E is described by the plane wave $\psi(\mathbf{r},t) = \exp\left[\frac{i}{h}(\mathbf{pr} - Et)\right]$, where h is Planck's constant. This dictates the form of operators of momentum and energy, $\hat{\mathbf{p}} = -ih\frac{\partial}{\partial \mathbf{r}}$, $\hat{E} = ih\frac{\partial}{\partial t}$, and the Schrödinger equation, $\hat{E}\psi = H(\hat{\mathbf{p}}, \mathbf{r}, t)\psi$, where H is the Hamilton function, which expresses the energy of a particle as function of momentum and time-spatial coordinates.

Consider now wave propagation in a 2D plane with Cartesian coordinates x, y, where the axis x is the preferable direction of wave propagation. If back scattering can be neglected then the wave problem can be reduced to a pseudo-differential or parabolic equation, where x plays the role of time. Plane waves have the following form:

$$u(x,y) = \exp\left[ik\left(\eta y + \sqrt{1-\eta^2}x\right)\right], \tag{1}$$

where $\left(\sqrt{1-\eta^2}, \eta\right)$ is the unity direction vector of the plane wave. This identifies η as the momentum conjugated with coordinate y and the Hamilton function for a vacuum equals $H = -\sqrt{1-\eta^2}$. If we describe waves in a medium with refractive index $n(x,y) = 1 + N(x,y)$, then the Hamilton function takes the form $H(\eta, y, x) = -\sqrt{n^2 - \eta^2}$. In multiple phase screen modeling (*Martin*, 1992; *Gorbunov and Gurvich*, 1998a; *Sokolovskiy*, 2001), the following approximations are used: (1) pseudo-differential approximation, $H(\eta, y, x) \approx -\sqrt{1-\eta^2} - N(x,y)$, and (2) parabolic approximation, $H(\eta, y, x) \approx -n(y,x) + \eta^2/2$. The momentum operator is then $\hat{\eta} = \dfrac{1}{ik}\dfrac{\partial}{\partial y}$, and the pseudo-differential equation is written as follows:

$$-\frac{1}{ik}\frac{\partial}{\partial x}u = H(\hat{\eta}, y, x)u. \tag{2}$$

This equation describes direct waves propagating in the nearly-x direction. It can also be derived by the operator factorization of the Helmholtz equation, which describes both direct and back scattered waves (*Martin*, 1992). In order to construct a short-wave asymptotic solution of this equation, the wave field is represented in the form $u(x,y) = A(x,y)\exp\left(ik\Psi(x,y)\right)$ (*Kravtsov and Orlov*, 1990). If we substitute this into Eq. (2) and expand it with respect to powers of k^{-1}, then the high-order terms (k^0) produce the Hamilton–Jacobi equation

$$-\frac{\partial \Psi}{\partial x} = H\left(\frac{\partial \Psi}{\partial y}, y, x\right), \tag{3}$$

whose characteristic lines (geometric optical rays) are described by the following canonical Hamilton system:

$$\frac{dy}{dx} = \frac{\partial H}{\partial \eta}, \qquad \frac{d\eta}{dx} = -\frac{\partial H}{\partial y}. \tag{4}$$

The phase along a ray is described by the differential equation $d\Psi = \eta\, dy - H\, dx$. The geometric optical amplitude $A(x,y)$ along a ray with initial condition y_0 is equal to $\varphi(x,y)/\sqrt{J(x,y)}$, where $J(x,y) = dy(x,y_0)/dy_0$, and the function φ is described by the transport differential equation integrated along the ray (*Mishchenko et al.*, 1990). For our approximate Hamilton functions, $\varphi = \text{const}$ along each ray, which means that energy defined as $E(x) = \int |u(x,y)|^2\, dy$ is conserved. The functions φ and J are defined on the ray manifold, and in multipath areas $\varphi(x,y)$ and $J(x,y)$ are multi-valued. On caustics, where $J(x,y) = 0$, the geometric optical amplitude goes to infinity and this solution does not work. Each ray is characterized by the coordinates (y, η) in the cross-section of the phase space related to some x.

Figure 1 shows an example of a ray manifold in the phase space. At point y_2 there are three rays, and for each of them $J_y(y) \neq 0$, therefore the wave field can be found as a superposition of three wave fields in the GO approximation. At point y_1 there is a caustic $(y_1, \eta_1(y_1))$, where two rays are degenerated into one and $J(x) = 0$, and there is also a ray $(y_1, \eta_2(y_1))$, where $J(x) \neq 0$.

In order to find the form of the asymptotic solution that works on caustics, we consider the Fourier transform of the wave field (momentum representation):

$$\tilde{u}(x,\eta) = F_{y\to\eta}u = \sqrt{\frac{-ik}{2\pi}} \int u(x,y) \exp\left(-iky\eta\right)\, dy. \tag{5}$$

We can also represent the transformed wave field in the form $\tilde{u}(x,\eta) = A'(x,\eta)\exp\left(ik\Psi'(x,\eta)\right)$. It can be found asymptotically using the stationary phase method (*Born and Wolf*, 1964). If $y_s(x,\eta)$ is the stationary phase point of the Fourier integral, then we have the following relationships:

$$\Psi'(x,\eta) = \Psi(x, y_s(x,\eta)) - y_s(x,\eta)\eta + \frac{\gamma}{k}, \tag{6}$$

$$\left.\frac{\partial\Psi(x,y)}{\partial y}\right|_{y_s(x,\eta)} = \eta, \tag{7}$$

$$\frac{\partial\Psi'(x,\eta)}{\partial\eta} = \frac{\partial y_s(x,\eta)}{\partial\eta}\left(\frac{\partial\Psi}{\partial y} - \eta\right) - y_s(x,\eta) = -y_s(x,\eta), \tag{8}$$

$$A'(x,\eta) = \frac{A(x,y_s(x,\eta))}{\sqrt{\left|-\dfrac{\partial^2\Psi}{\partial y^2}\right|}} = \frac{A(x,y_s(x,\eta))}{\sqrt{\left|-\dfrac{\partial\eta_s}{\partial y}\right|}} = A(x,y_s(x,\eta))\sqrt{\left|-\frac{\partial y_s}{\partial\eta}\right|} \tag{9}$$

where $\gamma = \pm\pi/4$, and $\eta_s(x,y)$ is the solution of the equation $y = y_s(x,\eta)$. The term γ/k in the eikonal asymptotically vanishes and it will be neglected. Equation (7) follows from the fact that at a stationary point the derivative of the phase of the integrand equals zero, and it shows that the stationary point $y_s(x,\eta)$ belongs to the ray manifold. Equation (8) indicates that if we use momentum as the new coordinate $y' = \eta$ and transform the wave field to the momentum representation, then the conjugated momentum is equal to $\eta' = -y$. We can also introduce the new Hamilton function $H'(\eta', y') = H(y', -\eta')$ and rewrite the canonical Hamilton system for rays in exactly the same form:

$$\frac{dy'}{dx} = \frac{\partial H'}{\partial\eta'}, \qquad \frac{d\eta'}{dx} = -\frac{\partial H'}{\partial y'}.$$

From equation (6) we can also derive the equation for the eikonal $d\Psi' = -y\,d\eta - H\,dx = \eta'\,dy' - H'\,dx$, and therefore we can also write the Hamilton–Jacobi equation for Ψ' in the coordinates (y', η') with Hamilton function H'.

From equation (9) we infer energy conservation when transforming to the momentum representation: $A'^2 d\eta = A^2 dy$ (this also explains the choice of the normalizing factor of $(-ik/2\pi)^{1/2}$ in the Fourier transform). Using this fact and conservation of energy along the rays mentioned above, we can infer that the wave problem can be formulated in the same way in the momentum representation, i.e.,

$$-\frac{1}{ik}\frac{\partial}{\partial x}\tilde{u} = H'(\hat{\eta}', y', x)\tilde{u}, \tag{10}$$

and the asymptotic solution will have the form $\tilde{u}(x,\eta) = \exp\left(ik\Psi'(x,\eta)\right)\varphi'(x,\eta)/\sqrt{J'(x,\eta)}$, where $J'(x,\eta) = d\eta(x,\eta_0)/d\eta_0$ and $\varphi'(x,\eta) = \varphi(x, y(x,\eta))$, where $\eta_0 = y'_0$ is the initial momentum (or new coordinate) of the ray.

This results in the following construction of the Maslov operator K (in Russian literature also referred to as the canonical operator). Given ray manifold and a normalized amplitude φ defined on the ray manifold the asymptotic solution $K\varphi$ is equal to the following expression:

$$K\varphi = \begin{cases} \dfrac{\exp\left(ik\Psi(x,y)\right)\varphi(x,y)}{\sqrt{J(x,y)}}, \text{ if } J(x,y) \neq 0, \\ F^{-1}_{\eta\to y}\dfrac{\exp\left(ik\Psi'(x,\eta)\right)\varphi'(x,\eta)}{\sqrt{J'(x,\eta)}}, \text{ if } J'(x,\eta) \neq 0, \end{cases} \tag{11}$$

where $F^{-1}_{\eta\to y}$ is the inverse Fourier transform.

Consider the ray manifold in Figure 1. At the point y_1 the solution will be the sum of two components, which we denote by the points of the ray manifold: (1) component from $(y_1, \eta_1(y_1))$ belongs to a caustic and it must be computed in the η-representation and Fourier-transformed to the y-representation; and (2) component from $(y_1, \eta_2(y_1))$ can only be computed in the y-representation, because it belongs to a caustic in the η-representation. At the point y_2 there are three components, and the first one $(y_2, \eta_1(y_2))$ must be computed in the y-representation, while the other two allow for both y and η-representations.

1.2.2 Fourier Integral Operators

Fourier Integral Operators arise when the Maslov operator is used for the derivation of the Green function of a wave propagation problem. The asymptotic solution in FIO form is based on the GO ray configuration, which defines the kernel of the FIO transforming the GO solution to a more accurate asymptotic solution. Given initial condition $u_0 = u(0, y)$, we will find the solution $u(x, z)$, where we introduce another notation z for the vertical coordinate for the propagated wave (a duplicate of the y-coordinate),

because in the further consideration it will be necessary to consider z a different coordinate in a different space. We use the plane wave expansion $\sqrt{ik/2\pi}\int \tilde{u}(0,\eta)\exp(iky\eta)d\eta$ and for each plane wave the asymptotic solution can be found in the form $[K\varphi](x,z,\eta)$. Then the solution can be written in the following form:

$$u(x,z) = \sqrt{\frac{ik}{2\pi}}\int [K\varphi](x,z,\eta)\tilde{u}(0,\eta)d\eta. \tag{12}$$

This is the general definition of the FIO (*Mishchenko et al.*, 1990). If the propagation of each plane wave can be described in coordinate representation, then the corresponding FIO can be written in the following form:

$$u(x,z) = \hat{\Phi}_1 u_0 = \sqrt{\frac{ik}{2\pi}}\int a_1(x,z,\eta)\exp(ikS_1(x,z,\eta))\tilde{u}(0,\eta)d\eta. \tag{13}$$

If propagation of each plane wave can be described in momentum representation then it is convenient to expand the wave field using the plane waves $\sqrt{ik/2\pi}\tilde{u}(0,-\eta)\exp(-iky\eta)$. After substituting it into the momentum form of the Maslov operator and cancelling direct and inverse Fourier transforms, the corresponding FIO will take the following form:

$$u(x,z) = \hat{\Phi}_2 u_0 = \sqrt{\frac{-ik}{2\pi}}\int a_2(x,z,y)\exp(ikS_2(x,z,y))u(0,y)dy. \tag{14}$$

Here, $a_{1,2}$ and $S_{1,2}$ are termed amplitude and phase functions of the FIOs, respectively. In the following we will refer to $\hat{\Phi}_1$ and $\hat{\Phi}_2$ as to FIOs of type 1 (FIO1) and type 2 (FIO2), respectively. We can introduce momenta η and ξ for ingoing and outgoing waves, respectively. Then equations for geometric optical rays can be written in the form $z = z(y,\eta), \xi = \xi(y,\eta)$. For the phase functions we can write the following geometric optical equations: $S_1(x,z,\eta) = y\eta + \Sigma_1(x,z,\eta)$ and $S_2(x,z,y) = \Sigma_2(x,z,y)$, where $\Sigma_{1,2}$ is the phase path along the ray between the points $(0,y)$ and (x,z), and $y\eta$ is the phase of the incident plane wave. Because wave fronts are normal to geometric optical rays, we can write the differential equation $d\Sigma_{1,2} = \xi\,dz - \eta\,dy$. Thus, we have the following differential equations for the phase functions (note, x is fixed):

$$dS_1 = \xi\,dz + y\,d\eta, \tag{15}$$

$$dS_2 = \xi\,dz - \eta\,dy. \tag{16}$$

The derivation of the amplitude functions $a_{1,2}$ uses the energy conservation in geometric optics. For the first type of FIO (13) we consider the stationary

phase approximation:

$$\hat{\Phi}_1 u_0 = \left. \frac{a_1(x,z,\eta) A'(0,\eta) \exp\left[ik\left(S_1(x,z,\eta) + \Psi'(0,\eta)\right)\right]}{\sqrt{\left| -\frac{\partial^2 S_1(x,z,\eta)}{\partial \eta^2} - \frac{\partial^2 \Psi'(0,\eta)}{\partial \eta^2} \right|}} \right|_{\eta=\eta(x,z)}, \quad (17)$$

where $\eta(x,z)$ is the stationary phase point determined by the equation:

$$\left. \frac{\partial S_1(x,z,\eta)}{\partial \eta} + \frac{\partial \Psi'(0,\eta)}{\partial \eta} \right|_{\eta=\eta(x,z)} = 0. \quad (18)$$

Energy conservation dictates that

$$\left. \frac{\left|a_1(x,z,\eta) A'(0,\eta)\right|^2}{\left| -\frac{\partial^2 S_1(x,z,\eta)}{\partial \eta^2} - \frac{\partial^2 \Psi'(0,\eta)}{\partial \eta^2} \right|} \right|_{\eta=\eta(x,z)} dz = \left|A'(0,\eta(x,z))\right|^2 \left|d\eta(x,z)\right|. \quad (19)$$

Here we also used the conservation of energy in the Fourier transform $A'^2 d\eta = A^2 dy$, which follows from Eq. (9). This indicates that the amplitude function must be equal to the following expression:

$$\left|a_1(x,z,\eta)\right|^2 = \left| -\frac{\partial^2 S_1(x,z,\eta)}{\partial \eta^2} - \frac{\partial^2 \Psi'(0,\eta)}{\partial \eta^2} \right|_{\eta=\eta(x,z)} \left| \frac{d\eta(x,z)}{dz} \right|. \quad (20)$$

Differentiating equation (18) with respect to z results in the following equation:

$$\left(\frac{\partial^2 S_1(x,z,\eta)}{\partial \eta^2} + \frac{\partial^2 \Psi'(0,\eta)}{\partial \eta^2} \right) \Bigg|_{\eta=\eta(x,z)} \frac{d\eta(x,z)}{dz} = - \left. \frac{\partial^2 S_1(x,z,\eta)}{\partial \eta \, \partial z} \right|_{\eta=\eta(x,z)}. \quad (21)$$

Replacing η with y, we can repeat the same derivation for the second type of FIO. Finally, we have the following expressions for the amplitude functions:

$$a_1(x,z,\eta) = \sqrt{\left| \frac{\partial^2 S_1(x,z,\eta)}{\partial z \, \partial \eta} \right|}, \quad (22)$$

$$a_2(x,z,y) = \sqrt{\left| \frac{\partial^2 S_2(x,z,y)}{\partial z \, \partial y} \right|}. \quad (23)$$

These expressions can also be derived from the requirement that $\hat{\Phi}^* = \hat{\Phi}^{-1}$, where $\hat{\Phi}^*$ is the conjugated operator (*Egorov*, 1985), which is equivalent to energy conservation.

1.2.3 Canonical Transforms

Now we will discuss the connection between FIOs and canonical transforms. Consider the phase space with coordinate y and momentum η and assume that the dynamics is described by the Hamilton function $H(\eta, y)$. We can parameterize the same phase space by another coordinate z and momentum ξ and define a new Hamilton function $H'(z, \xi)$ in such a way that

$$dS_1 = \xi\, dz + y\, d\eta - (H' - H)dx, \tag{24}$$

$$dS_2 = \xi\, dz - \eta\, dy - (H' - H)dx. \tag{25}$$

Then the same dynamics can also be described in the new coordinates with the new Hamilton function. This type of coordinate transform in the phase space is termed a canonical transform, with $S_1(x, z, \eta)$ and $S_2(x, z, y)$ being different types of its generating functions (*Arnold*, 1978). The geometric optical solution of a wave problem can be written in different canonical coordinates. We can also ask: is it possible to reformulate the wave problem in the new phase space with the new Hamilton operator? This question was first studied by *Egorov* (1985); *Egorov et al.* (1999), who showed that the FIO of the first type maps the wave field to the new representation. Below we show that the FIO of the second type can also be used for the same purpose. We will derive the formula for the commutation of a FIO of the second type and a pseudo-differential operator $P(\hat{\eta}, y)$, which is defined as follows $P(\hat{\eta}, y)u = F^{-1}_{\eta\to y}\left[P(\eta, y)\tilde{u}(\eta)\right]$, where $P(\eta, y)$ is termed the symbol of the operator. We can write $\hat{\Phi}_2 P(\hat{\eta}, y) = Q(\hat{\xi}, z)\hat{\Phi}_2$, where $Q(\hat{\xi}, z)$ is the representation of operator $P(\hat{\eta}, y)$ in the new coordinates and $\hat{\xi} = \dfrac{1}{ik}\dfrac{\partial}{\partial z}$ is the new momentum operator. First, we compute $\hat{\Phi}_2 P(\hat{\eta}, y)u$ as follows:

$$\begin{aligned}
\hat{\Phi}_2 P(\hat{\eta}, y)u &= \sqrt{\frac{ik}{2\pi}} \int a_2(x, z, y) \exp(ikS_2(x, z, y)) \times \\
&\quad \times \frac{k}{2\pi} \int\int P(\eta, y) \exp(ik(y - \bar{y})\eta) u(\bar{y})\, d\bar{y}\, d\eta\, dy = \\
&= \sqrt{\frac{ik}{2\pi}} \int \frac{k}{2\pi} \int\int P(\eta, y) \exp\left[ik(y - \bar{y})\left(\eta + \frac{\partial S_2}{\partial y}\right)\right] dy\, d\eta \times \\
&\quad \times a_2(x, z, \bar{y}) \exp(ikS_2(x, z, \bar{y}))u(\bar{y})\, d\bar{y} = \\
&= \sqrt{\frac{ik}{2\pi}} \int P\left(-\frac{\partial S_2}{\partial y}, \bar{y}\right) a_2(x, z, \bar{y}) \exp(ikS_2(x, z, \bar{y}))u(\bar{y})\, d\bar{y}.
\end{aligned} \tag{26}$$

Here we used the asymptotic formula: $(k/2\pi)\int\int f(y, \eta) \exp(iky\eta)\, dy\, d\eta = f(0, 0)$ (*Egorov*, 1985; *Egorov et al.*, 1999), which can be easily derived by

Tailor expansion of $f(y,\eta)$. Next, the operator $Q(\hat{\xi},z)\hat{\Phi}_2$ can be evaluated as follows:

$$Q(\hat{\xi},z)\hat{\Phi}_2 u = \sqrt{\frac{ik}{2\pi}}\int Q\left(\frac{\partial S_2}{\partial z},z\right) a_2(x,z,y)\exp(ikS_2(x,z,y))u(y)\,dy. \quad (27)$$

From this we obtain that $P\left(-\frac{\partial S_2}{\partial y},y\right) = Q\left(\frac{\partial S_2}{\partial z},z\right)$. Our consideration is similar to that given by *Egorov* (1985), who proved that for FIOs of the first type: $Q(\frac{\partial S_1}{\partial z},z) = P(\eta,\frac{\partial S_1}{\partial \eta})$. Because $-\frac{\partial S_2}{\partial y}=\eta$, $\frac{\partial S_2}{\partial z}=\frac{\partial S_1}{\partial z}=\xi$, $\frac{\partial S_1}{\partial \eta}=y$, we see that in both cases it follows that $Q(\xi,z)=P(\eta(\xi,z),y(\xi,z))$. If we redefine (pseudo-) differential operators in the representation of the new coordinate z and momentum ξ (this transform mixes coordinates and conjugated differential operators), then the wave function in this representation equals $\hat{\Phi}_{1,2}u$. The wave equation can then be rewritten in the new coordinates as follows:

$$H'(\hat{\xi},z,x)\hat{\Phi}_{1,2}u = -\frac{1}{ik}\frac{\partial}{\partial x}\hat{\Phi}_{1,2}u = -\frac{\partial S_{1,2}}{\partial x}\hat{\Phi}_{1,2}u + \hat{\Phi}_{1,2}\left(-\frac{1}{ik}\frac{\partial}{\partial x}u\right) =$$
$$= -\frac{\partial S_{1,2}}{\partial x}\hat{\Phi}_{1,2}u + \hat{\Phi}_{1,2}H(\hat{\eta},y,x)u = -\frac{\partial S_{1,2}}{\partial x}\hat{\Phi}_{1,2}u + H(\eta(\hat{\xi},z),y(\hat{\xi},z),x)\hat{\Phi}_{1,2}u. \quad (28)$$

From this we obtain that, in agreement with Eqs. (24)-(25): $H' = -\partial S_{1,2}/\partial x + H$. Therefore the technique of FIO generalizes the technique of Maslov operators. Maslov operators use a special canonical transform ($z=\eta$, $\xi=-y$; $\pi/2$-rotation of phase plane), while FIOs are associated with a wide class of canonical transforms. This has a big advantage, because it may allow for writing the global solution of a wave problem in a situation where the Maslov operator would require sewing together local solutions in order to obtain a global solution. Another important advantage is that FIOs can be used for solving inverse problem of reconstruction of the ray structure of wave fields.

1.3 Processing Radio Occultations

1.3.1 Canonical Transform without Back Propagation

We will now consider the complex field $u(y) = A(y)\exp(ik\Psi(y))$ recorded along the observation trajectory parameterized with some coordinate y, which can be e.g. time, arc length, or satellite-to-satellite angle θ (*Jensen et al.*, 2003). For circular satellite orbits, and choosing $y=\theta$, we obtain $\dot{\Psi} = p\dot{\theta} = p$,

where p is the ray impact parameter. Here and in the following the dot denotes a full derivative with respect to the trajectory parameter y. In the momentum representation, the wave function is $\tilde{u}(p) = A'(p)\exp(ik\Psi'(p))$, and the derivative of its eikonal $d\Psi'(p)/dp$ is equal to satellite-to-satellite angle $\theta_s(p)$ of the trajectory point, where the ray with impact parameter p was observed (*Jensen et al.*, 2003).

For generic, non-circular orbits, *Gorbunov and Lauritsen* (2002) suggested processing radio occultation data by a generic Fourier integral operator (14) of the second type. Below we present the derivation of its amplitude function $a_2(p, y)$ and phase function $S_2(p, y)$. The expression for the phase function was first obtained by *Jensen et al.* (2004). From Eq. (25) it follows that

$$\frac{\partial S_2(p,y)}{\partial y} = -\eta(p,y), \tag{29}$$

where $\eta(p, y)$ is equal to the derivative of the eikonal of the geometric optical ray with given impact parameter p observed at the trajectory point y. If y is chosen to be equal to the time t, then $\eta = -\Delta\omega/k$, where $\Delta\omega$ is the Doppler frequency shift (we assume the time dependence of the wave field in the form $A(y)\exp(ik\Psi(y) - i\omega t)$). The function $\eta(p, y)$ is computed using the geometrical optics. This equation will be used for the definition of the phase function $S_2(p, y)$.

The derivative of the eikonal of the transformed wave field $\hat{\Phi}_2 u(p)$ is evaluated as follows:

$$\frac{\partial \Psi'(p)}{\partial p} = \left.\frac{\partial S_2(p,y)}{\partial p}\right|_{y=y_s(p)} = \xi(p, y_s(p)). \tag{30}$$

Thus, equation (25) has a very simple interpretation: We probe some value of impact parameter p and integrate the expression $\exp(ikS_2(p, y) + ik\Psi(y)))$. Because $k\partial S_2/\partial y$ equals the Doppler frequency $-k\eta(p, y)$ for the ray at a given trajectory point y with given impact parameter p, the oscillating kernel $\exp(ikS_2(p, y))$ locates geometric optical rays, which correspond to stationary phase points of the integral operator. At a stationary phase point, the term $-k\int \eta\, dy$ in the phase of the kernel is reduced by the term kΨ in the phase of the wave field. The remaining term $k\int \xi\, dp$ in the phase determines the derivative ξ of the phase of the transformed wave field.

1.3.2 Phase Function

The phase function can be derived using equation (29). We will use the following expression for the derivative of the phase path:

$$\dot{\Psi} = \eta(p,y) = p\dot{\theta} + \frac{\dot{r}_G}{r_G}\sqrt{r_G^2 - p^2} + \frac{\dot{r}_L}{r_L}\sqrt{r_L^2 - p^2}, \tag{31}$$

where r_G and r_L are GPS and LEO (or, generally, transmitter and receiver) satellite radii. Here and in the following, r_G, r_L, and θ are functions of the trajectory parameter y. The expression for the phase function (*Jensen et al.*, 2004) can then be found by integrating $\eta(p, y)$ over y for a fixed value of impact parameter p:

$$\begin{aligned} S_2(p,y) &= -\int \left(p\dot{\theta} + \frac{\dot{r}_G}{r_G}\sqrt{r_G^2 - p^2} + \frac{\dot{r}_L}{r_L}\sqrt{r_L^2 - p^2} \right) dy = \\ &= -\int \left(p\, d\theta + \frac{dr_G}{r_G}\sqrt{r_G^2 - p^2} + \frac{dr_L}{r_L}\sqrt{r_L^2 - p^2} \right) = \\ &= -p\theta - \sqrt{r_G^2 - p^2} + p \arccos\frac{p}{r_G} - \sqrt{r_L^2 - p^2} + p \arccos\frac{p}{r_L}, \end{aligned} \tag{32}$$

where one can add an arbitrary function $f(p)$, which we take to equal 0. Refraction angle can be expressed as a function of trajectory parameter y, which defines the satellite positions, and impact parameter p, which defines the directions of emerging and incident rays:

$$\epsilon(p, y) = \theta - \arccos\frac{p}{r_G} - \arccos\frac{p}{r_L}\,. \tag{33}$$

Then we can express the derivative of the eikonal of the transformed wave field as follows (*Jensen et al.*, 2004):

$$\xi(p, y) = -\theta + \arccos\frac{p}{r_G} + \arccos\frac{p}{r_L} = -\epsilon(p, y). \tag{34}$$

For the reconstruction of the refraction angle profile from the measurements of the wave field along the orbit we apply the FIO2 operator (14), which produces a function $\hat{\Phi}_2 u(p) = A'(p)\exp(ik\Psi'(p))$ of impact parameter p. The derivative of its eikonal $\Psi'(p)$ with a negative sign is then equal to the refraction angle $\epsilon = \epsilon(p, y_s(p))$, where $y_s(p)$ is the coordinate of the trajectory point, where the ray with impact parameter p was observed ($y_s(p)$ is the stationary point of oscillating integral (14)).

For a circular occultation geometry ($r_G = \text{const}$, $r_L = \text{const}$, $\dot{\theta} = \text{const}$) the phase function reads $S_2(p, y) = -p\theta + F(p)$, and the FIO is reduced to the Fourier transform. In the FSI method, the phase function $S_2(p, y)$ is equal to $-p\theta$. The derivative of the phase is then equal to $-\theta$, and refraction angle can be found as function of θ and p using equation (33) ($\epsilon = \theta + F'(p)$).

From the consideration of the oscillating kernel $\exp(ikS_2(p, y))$, the following relationship can be inferred:

$$S_2(p, y_s(p)) = -\Psi(p) + \int_p^\infty \epsilon(p')\, dp'. \tag{35}$$

This relationship can also be derived directly by computing phase path $\Psi(p) = \int n\, ds$, where the integral is taken along the ray with impact parameter p in a spherically-layered medium with refractive index $n(r)$.

1.3.3 Amplitude Function

The amplitude function $a_2(p, y)$ of the FIO does not play any role in the computation of refraction angles. For example, we could set $a_2(p, y) \equiv 1$. However, the correct definition of the amplitude of the transformed wave field is necessary for the retrieval of atmospheric absorption (*Gorbunov*, 2002a; *Jensen et al.*, 2004) (also M. S. Lohmann, A. S. Jensen, H.-H. Benzon, A. S. Nielsen, *Computation of atmospheric absorption by the FSI technique*, manuscript in preparation, 2003). *Gorbunov* (2002a) discussed the possibility of retrieving the atmospheric absorption from the amplitude of the transformed wave field in the framework of the standard CT method and it was shown that in the absense of absorption the CT amplitude is very close to a constant. Indeed, the CT amplitude describes the distribution of energy with respect to impact parameters. The transmitted energy is homogeneously distributed over spatial transmission angle. For an immovable transmitter and 2D case the CT amplitude is proportional to $(d\psi_G/dp)^{1/2}$, where ψ_G is the angle between outgoing ray and GPS radius. For GPS-LEO occultations, where the distance from the transmitter to the planet limb is big, it is a good approximation to assume a homogeneous distribution of transmitted energy with respect to impact parameters. For LEO-LEO occultations, the accuracy of this approximation is worse. *Jensen et al.* (2004) discussed normalizing the amplitude to the distribution of the transmitted energy with respect to impact parameters. Our consideration follows that given by *Jensen et al.* (2004) with some generalizations and refinements: we consider both 2D and 3D cases, use more accurate derivation of the amplitude and parameterize trajectory with coordinate y instead of θ.

For the derivation of the amplitude function $a_2(p, y)$, we use energy conservation. We can write an equation similar to Eq. (19) for the coordinate y, amplitude A, eikonal Ψ, and amplitude function a_2. For Cartesian coordinate y, we defined infinitesimal element of energy as $|u(x, y)|^2\, dy$. For a generic coordinate y, we must introduce a measure μ and replace dy with μdy. The measure will be used in the local formulation of energy conservation and will be understood as a function $\mu(p, y)$. Using the expression (32) for the phase function derived above we arrive at the following expression for

the amplitude function:

$$a_2(p,y) = \sqrt{\mu \left| \frac{\partial^2 S_2(p,y)}{\partial p \, \partial y} \right|} = \left| \mu \left(\dot{\theta} - \frac{\dot{r}_G}{r_G} \frac{p}{\sqrt{r_G^2 - p^2}} - \frac{\dot{r}_L}{r_L} \frac{p}{\sqrt{r_L^2 - p^2}} \right) \right|^{1/2}. \tag{36}$$

For the definition of the measure μ we consider the energy conservation in geometrical optics. We consider an infinitesimal ray tube for given satellite positions. The amplitude A is defined by the requirement that $dE_R \equiv A^2 \cos\psi \, dS = dE_T$, where dE_R is the energy received in the aperture dS, ψ is the angle between the ray tube and the normal to the aperture, dE_T is the transmitted energy inside the ray tube. Because the GO amplitude A only depends on r_G, r_L, and θ, rather than on satellite velocities, we can consider any virtual receiving aperture. If it is chosen to be an infinitesimal element of the sphere ($r_{L,G} = \text{const}$), then we can write the distribution of transmitted and received energy, E_T and E_R, respectively (*Eshleman et al.*, 1980; *Jensen et al.*, 2003, 2004) (also S. Leroy, *Amplitude of an Occultation Signal in Three Dimensions*, unpublished manuscript, 2001).

$$\begin{aligned} dE_T &= \frac{P}{2\pi} d\psi_G \left\{ \frac{1}{2} \sin\psi_G d\phi \right\}_{3D} = \frac{P}{2\pi} \frac{1}{\sqrt{r_G^2 - p_G^2}} \left\{ \frac{1}{2} \frac{p_G}{r_G} d\phi \right\}_{3D} \frac{dp_G}{dp} dp, \\ dE_R &= A^2 r_L \cos\psi_L \left\{ \frac{1}{2} r_L \sin\theta d\phi \right\}_{3D} \delta\theta = \\ &= A^2 \sqrt{r_L^2 - p_L^2} \left\{ \frac{1}{2} r_L \sin\theta d\phi \right\}_{3D} \frac{\delta\theta}{dy} dy, \end{aligned} \tag{37, 38}$$

where terms is curly brackets $\{...\}_{3D}$ relate to the 3D case, P is the transmitter power, ϕ is the angle of rotation around the axis from the curvature center to the transmitter, $\psi_{G,L} = \arcsin(p/r_L)$ are the angles between the ray and satellite radii at the transmitter and receiver, $p_{G,L} = r_{L,G} \sin\psi_{L,G}$ are impact parameters at transmitter and receiver, A is the geometric optical amplitude of a received ray, and $\delta\theta$ is the virtual variation of the satellite-to-satellite angle along the sphere ($r_{L,G} = \text{const}$). For a spherically symmetrical atmosphere $p_{G,L} = p$, for a non-spherical atmosphere p is computed from the Doppler frequency shift (*Vorob'ev and Krasil'nikova*, 1994), and therefore p is a function of p_G and p_L. Because ψ_L is the angle between a ray and the normal to the virtual circular orbit (rather than the real satellite orbit) it should be used in combination with the virtual infinitesimal element of the sphere $\delta\theta$ (cf. the use of $d\theta$ computed along the real trajectory by *Jensen et al.* (2003)). This allows for the definition of the measure such that

$(P/2\pi)dp = A^2\mu dy$ (under the assumption of spherical symmetry):

$$\mu = \sqrt{r_L^2 - p^2}\sqrt{r_G^2 - p^2}\left\{\frac{r_L r_G}{p}\sin\theta\right\}_{3D}\frac{\delta\theta}{dy}. \tag{39}$$

For the definition of the virtual variation $\delta\theta$ we can write:

$$\delta\theta = d\theta - \left(\frac{\partial\theta}{\partial r_G}\right)_p dr_G - \left(\frac{\partial\theta}{\partial r_L}\right)_p dr_L = d\theta - \frac{dr_G}{r_G}\frac{p}{\sqrt{r_G^2 - p^2}} - \frac{dr_L}{r_L}\frac{p}{\sqrt{r_L^2 - p^2}}, \tag{40}$$

where we used equation (33). Finally, we can write the following expression for the amplitude function:

$$a_2(p,y) = \left(\sqrt{r_L^2 - p^2}\sqrt{r_G^2 - p^2}\left\{\frac{r_L r_G}{p}\sin\theta\right\}_{3D}\right)^{1/2} \times \\ \times\left(\dot\theta - \frac{\dot r_G}{r_G}\frac{p}{\sqrt{r_G^2 - p^2}} - \frac{\dot r_L}{r_L}\frac{p}{\sqrt{r_L^2 - p^2}}\right). \tag{41}$$

1.3.4 Representation of Approximate Impact Parameter

The FIO defined by the phase and amplitude functions (32) and (41), respectively, solves the problem of the extraction of refraction angles from measurements of the complex field along a satellite trajectory, directly without back propagation. However, this operator cannot be implemented as a Fourier transform and therefore its numerical implementation, especially for high frequencies such as 10-30 GHz, is slow. Here we shall describe an approximation that allows for writing the FIO2 operator in the form of a Fourier transform.

Consider the measured complex field $u(t) = A(t)\exp(ik\Psi(t))$ and corresponding momentum $\sigma = d\Psi/dt$. We use a FIO associated with the canonical transform from the (t,σ) to the (p,ξ)-representation. The impact parameter p is a function of t,σ: $p = p(t,\sigma)$. Instead of exact impact parameter we introduce its approximation $\tilde p$:

$$\begin{aligned}\tilde p(t,\sigma) &= p_0(t) + \frac{\partial p_0}{\partial\sigma}(\sigma - \sigma_0(t)) = f(t) + \frac{\partial p_0}{\partial\sigma}\sigma,\\ f(t) &= p_0(t) - \frac{\partial p_0}{\partial\sigma}\sigma_0(t),\end{aligned} \tag{42}$$

where $\sigma_0(t)$ is a smooth model of Doppler frequency, $p_0(t) = p(\sigma_0(t),t)$, and $\partial p_0/\partial\sigma = \partial p/\partial\sigma|_{\sigma=\sigma_0(t)}$. We compute $\sigma_0(t)$ by differentiation of the eikonal with a strong smoothing over approximately 2 s time interval. We now parameterize the trajectory with the coordinate $Y = Y(t)$, where we use the

notation Y in order to distinguish between this specific choice of the trajectory coordinate and the generic coordinate y. For brevity we use the notation $u(Y)$ instead of $u(t(Y))$. For the coordinate Y and the corresponding momentum η we use the following definitions:

$$\begin{aligned} dY &= \left(\frac{\partial p_0}{\partial \sigma}\right)^{-1} dt = \frac{\partial \sigma}{\partial p_0} dt, \\ \eta &= \frac{\partial p_0}{\partial \sigma}\sigma. \end{aligned} \tag{43}$$

Then, we can write the following linear canonical transform:

$$\begin{aligned} \tilde{p} &= f(Y) + \eta, \\ \xi &= -Y, \end{aligned} \tag{44}$$

where we use the notation $f(Y)$ instead of $f(t(Y))$. The generating function of this canonical transform is easily computed from the differential equation $dS_2 = \xi\, d\tilde{p} - \eta\, dY = -Y\, d\tilde{p} - (\tilde{p} - f(Y))\, dY$:

$$S_2(\tilde{p}, Y) = -\tilde{p}Y + \int_0^Y f(Y')\, dY'. \tag{45}$$

Using equation (31) we can find $\partial\sigma/\partial p$ and therefore dY:

$$dY = d\theta - \frac{dr_G}{r_G}\frac{p_0}{\sqrt{r_G^2 - p_0^2}} - \frac{dr_L}{r_L}\frac{p_0}{\sqrt{r_L^2 - p_0^2}} \approx \delta\theta. \tag{46}$$

So we can approximately write $\delta\theta/dY \approx 1$. An accurate expression can be easily derived using Eq. (40), but we do not use it, because the accuracy of the above approximation is sufficient. Because $|\partial^2 S_2/\partial\tilde{p}\partial Y| = 1$, the amplitude function (36) equals $\sqrt{\mu}$ and it can be written as follows:

$$a_2(\tilde{p}, Y) = \left(\sqrt{r_L^2 - \tilde{p}^2}\sqrt{r_G^2 - \tilde{p}^2}\left\{\frac{r_L r_G \sin\theta}{\tilde{p}}\right\}_{\mathrm{3D}}\right)^{1/2}. \tag{47}$$

The amplitude function $a_2(\tilde{p}, Y)$ in the FIO can be replaced with $a_2(\tilde{p}, Y_s(\tilde{p}))$ and factored out from within the integral. The resulting operator can be written as the composition of adding a model, $ik\int f(Y)dY$, to the phase, the Fourier transform, and an amplitude factor:

$$\hat{\Phi}_2 u(\tilde{p}) = \sqrt{\frac{-ik}{2\pi}} a_2(\tilde{p}, Y_s(\tilde{p})) \int \exp\left(-ik\tilde{p}Y\right) \exp\left(ik\int_0^Y f(Y')\, dY'\right) u(Y)\, dY. \tag{48}$$

The function $Y_s(\tilde{p})$ equals $-\xi$, where the momentum ξ is the derivative of the eikonal of the integral term in (48). This operator maps the wave field to the representation of the approximate impact parameter $\tilde{p}$. Using equation (42), the exact value of σ and therefore impact parameter $p(\sigma, t)$ can be found from $\tilde{p}$, as a function $p(\tilde{p})$. Practically, however, the difference between exact and approximate impact parameters, p and $\tilde{p}$, is small and can be neglected.

The introduced FIO2 mapping (48) generalizes the FSI method (*Jensen et al.*, 2003): FSI uses a composition of a phase model with Fourier transform with respect to angle θ. Our definition of the coordinate Y takes into account the generic occultation geometry (and for circular orbits $Y = \theta$). We also use a more accurate derivation of the amplitude function a_2. We shall refer to this CT inversion technique based on the FIO of the second type as the CT2 algorithm.

1.4 Direct Modeling

Fourier integral operators can also be used for asymptotic direct modeling (*Gorbunov*, 2003). The FIOs $\hat{\Phi}_{1,2}$ with amplitude functions (22) and (23) can be easily inverted: $\hat{\Phi}_{1,2}^{-1} = \hat{\Phi}_{1,2}^{*}$. For example, $\hat{\Phi}_2^{-1}$ is a FIO2 with phase function $S_2^*(y,p) = -S_2(p,y)$ and amplitude function $a_2^*(y,p) = a_2(p,y)$. If the amplitude function equals $a_2 = \left(\mu\, \partial^2 S_2/\partial\tilde{p}\partial y\right)^{1/2}$, then the inverse operator can be approximately written with amplitude function $a_2^* = \left(\mu^{-1}\, \partial^2 S_2/\partial\tilde{p}\partial y\right)^{1/2}$, because μ is a slowly-changing function (the amplitude function at the stationary point can be factored out and the μ and μ^{-1} in the composition of the direct and inverse transform will cancel).

If we use the representation of approximate impact parameter $\tilde{p}$, then the direct model is especially efficient. Given a 3D atmospheric model, we first perform geometric optical modeling, and iteratively find the trajectory point $Y_s(\tilde{p})$, where the ray with the impact parameter $p(\tilde{p})$ is observed. The wave function in the $\tilde{p}$-representation is then equal to $w(\tilde{p}) = A'(\tilde{p}) \exp\left(-ik \int Y_s(\tilde{p}) d\tilde{p}\right)$, where the amplitude $A'(\tilde{p})$ equals a normalizing constant in the light zone and 0 in the geometric optical shadow. This function is then mapped into the Y-representation by the inverse FIO2:

$$u(Y) = \sqrt{\frac{ik}{2\pi}} \exp\left(-ik \int_0^Y f(Y')\, dY'\right) \int \exp(ik\tilde{p}Y)\, a_2^*(Y_s(\tilde{p}), \tilde{p})\, w(\tilde{p}) d\tilde{p}, \tag{49}$$

$$a_2^*(Y, \tilde{p}) = \left(\frac{1}{\sqrt{r_L^2 - p_L^2}\sqrt{r_G^2 - p_G^2}} \left\{\frac{p_G}{r_L r_G \sin\theta}\right\}_{3\mathrm{D}} \frac{dp_G}{d\tilde{p}}\right)^{1/2}, \tag{50}$$

where p_L and p_G are functions of $\tilde{p}$ computed for given atmosphere and satellite trajectories. For modeling atmospheric absorption, the amplitude $A'(\tilde{p})$ must also be multiplied by a factor of $\exp\left(-k\int n''ds\right)$, where n'' is the imaginary part of refractive index, and the integral is taken along the ray with the impact parameter $p(\tilde{p})$.

This technique of direct modeling has the following limitation of applicability: the approximate impact parameter $\tilde{p}$ must be an unique coordinate of the ray manifold. Another restriction of the asymptotic technique (for both inverse and direct modeling) is that diffraction inside the atmosphere is neglected (*Gorbunov et al.*, 2004).

Gorbunov (2003) discussed the inversion of the standard BP+CT composition based on the FIO of the first type for direct modeling. The wave function in the p-representation equals $w(p) = A'(p)\exp\left(ik\int\xi(p)dp\right)$, where ξ is the geometric optical momentum, and the amplitude for the 2D case and immovable transmitter was taken to equal $A_0\left(d\psi_G/dp\right)^{1/2}$, so that A^2dp is the infinetsimal element of transmitted energy. Then, $\hat{\Phi}_1^{-1}w$ is equal to the wave field along a vertical line, and it can be forward-propagated to the LEO orbit using the diffractive integral. The draw-backs of this algorithm are (1) the necessity of the forward propagation, which may be time-consuming for high frequencies and (2) the modeling of immovable transmitter only. The technique based on $\hat{\Phi}_2^{-1}$ suggested in this paper, is free from these disadvantages: it requires only one FFT, which is much faster than the computation of diffractive integrals, and it allows for modeling simultaneous movement of the transmitter and receiver, which is important for LEO-LEO occultations.

Simulation of moving transmitter and receiver was also discussed by *Mortensen et al.* (1999), who used an approximation based on the composition of geometrical optics and the thin screen approximation. However, their technique proved extremely time-consuming (for each sample of simulated data, it requires geometric optical propagation from transmitter and receiver to points of an intermediate thin screen and computation of one diffractive integral). Besides, it only works above 4 km (*Mortensen et al.*, 1999).

1.5 Numerical Simulations

Here, we compare the performance of the CT2 inversion technique introduced above and the standard composition of BP and CT techniques. For this purpose, we modelled a spherically symmetric atmosphere using a high-resolution tropical radio sonde profile of refractivity. We simulated radio occultation signals using multiple phase screens (MPS) for the standard GPS frequencies. The occultation model included an immovable transmitter and a receiver moving along a circular orbit. The MPS simulation followed the

scheme described e.g. by *Gorbunov and Gurvich* (1998a); *Sokolovskiy* (2001): the signal is propagated through the atmosphere using parallel phase screens, and from the last phase screen to the satellite orbit it is propagated using the diffractive integral. We used 2D formulas for the amplitude. The screen-to-screen step was 5 km, and the integration step for geometric optical modeling was 2.5 km. The simulated radio occultation signals were processed by the two inversion algorithms and the results of the reconstruction of refraction angle profile were compared with the exact geometric optical solution. The comparison presented in Figure 2 indicates a very good agreement between both inversion algorithms and the geometric optical solution. All the differences are in small scales below 50 m, which cannot be effectively resolved for the GPS frequencies, due to diffraction inside the atmosphere (*Gorbunov et al.*, 2004).

For the validation of the asymptotic direct modeling we performed numerical simulations with a simple spherically-symmetrical phantom (exponential model with a quasi-periodical perturbation):

$$n(z) = 1 + N_0 \exp\left(-\frac{z}{H}\right)\left[1 + \alpha\cos\left(\frac{2\pi z}{h}\right)\exp\left(-\frac{z^2}{L^2}\right)\right], \qquad (51)$$

where z is the height above the Earth's surface, $N_0 = 300 \times 10^{-6}$ is the characteristic refractivity at the Earth's surface (300 N-units), $H = 7.5$ km is the characteristic vertical scale of refractivity field, $\alpha = 0.003$ is the relative magnitude of the perturbation, $h = 0.3$ km is the period of the perturbation, $L = 3.0$ km is the characteristic height of the perturbation area. This phantom was smoothly sombined with the MSIS climatological model above 20 km.

We simulated radio occultation signals using MPS and the asymptotic solution for the frequency 9.7 GHz, which is intended to be used in LEO-LEO occultations. The results of the comparison of the amplitude of the simulated wave field for these two modeling techniques are presented in Figure 3. The peculiarity of the amplitude around 28.5 s is due to the transfer from MSIS to the test phantom. Between 40 and 47.5 s the amplitude indicates large-scale oscillations reproducing the oscillations of the refractivity profile. In this area there is no multipath propagation. After 47.5 s we notice increasing small-scale scintillations due to emergency of multipath propagation. The occultation fragment from 57 to 59 s with strong multipath scintillations is enlarged and shown separately. Figure 3 illustrates a good agreement of both these simulation techniques.

The asymptotic modeling is significantly faster than MPS modeling. One run of the asymptotic propagator took 4 minutes, while the MPS modeling

took 2 hours on a system based on a Pentium-III processor (1 GHz). For multiple channels, the computational time for MPS simulations is proportional to the number of channels. In the asymptotic propagator, the most time-consuming part is the geometric optical modeling, which is common for all the channels. The computation of an FFT with $2^{21} = 2097152$ points, which is required for the simulation of a 22.6 GHz channel, takes 3 s. Therefore, when simulating 3 channels, the asymptotic propagator will take approximately the same time, 4 minutes, while an MPS simulation will require 6 hours.

Figure 4 shows the geometric optical refraction angle profile and the results of the inversion of the simulated data. We present four combinations of the two simulation techniques: (1) the FIO asymptotic solution and (2) multiple phase screens; and the two inversion techniques: (1) CT2 and (2) the standard combination of BP and CT. This Figure shows good agreement between the GO solution and the retrieved refractivity profile. The strongest deviations of retrieved refraction angles from the reference GO profile are observed for processing MPS simulations in the lowest 200 m. This can be accounted for by the diffraction on the Earth's surface.

2 Conclusions on utility of Fourier Integral Operators for RO

FIOs are a very efficient means of analysis of wave fields. These operators describe short-wave asymptotic solutions of wave equations. Furthermore, these operators are linked to canonical transforms because the dynamics of geometric optical rays is also described by a canonical transform. The canonical Hamilton system describing geometric optical rays can be written in different canonical coordinates (coordinate and momentum). Because momentum is associated with a differential operator, a canonical transform can also be understood as a transform of the Hamilton operator of the wave problem.

The FIO associated with the canonical transform maps the wave field to the representation of the new canonical coordinates, and the wave equation can be asymptotically rewritten in the new representation. This makes this technique valuable for the inverse problem of the reconstruction of the ray manifold of a wave problem. Using impact parameter as a new coordinate, it is possible to map the wave function into the impact parameter representation. If impact parameter is a unique coordinate in the ray space, then in this representation there is no multipath and the momentum is equal to the derivative of the eikonal. The momentum is a function of ray direction or refraction angle. Previously, the technique of FIOs was applied in the composition with back propagation. However, it is possible to apply FIOs directly to radio occultation data measured along the LEO orbit, without BP. This technique allows for a very effective numerical implementation based on a single Fourier transform (CT2).

Another application of FIOs is the direct modeling. The asymptotic solution of the direct problem uses the mapping of the geometric optical solution in the impact parameter representation to the standard coordinate representation. The method based on the inverse CT2 is very efficient numerically because it can be implemented as the composition of the geometric optical solution and a single Fourier transform. This is important for direct modeling and processing radio occultation data at high frequencies (10-30 GHz), where the computation of diffractive integrals may be numerically very slow.

3 Asymptotic methods of modeling the propagation of centimeter waves in the atmosphere on limb paths

3.1 Introduction

Radio occultation (RO) data obtained by sounding of the Earth's atmosphere by signals of global navigation satellite systems have a large potential for applications in numerical weather prediction and tracking of global climate change (*Hajj et al.*, 2002). The optimal utilization of RO data is achieved by applying the most advanced data processing methods (*Gorbunov*, 2002a; *Jensen et al.*, 2003, 2004; *Gorbunov and Lauritsen*, 2004; *Hocke et al.*, 1999; *Igarashi et al.*, 2000). The development of advanced data processing algorithms always requires testing their capabilities on artificial data. Therefore, it is essential to have both accurate and efficient techniques for generating such data. Besides, realistic artificial data are necessary for ground-based tests of receivers intended for RO measurements. Artificial RO data are generated from global gridded fields of meteorological parameters and satellite trajectories by modeling the propagation of radio waves in the atmosphere. From the fields of meteorological parameters, a gridded refractive index field is computed, which is then interpolated.

Modeling of the wave propagation in the atmosphere is usually performed by the multiple phase screens (MPS) method (*Martin*, 1992). However, if the model field of the atmospheric meteorological parameters does not include small-scale inhomogeneities, the modeling can be performed by using asymptotic solutions based on the theory of Maslov operators or Fourier Integral Operators (FIO) (*Maslov and Fedoriuk*, 1981; *Mishchenko et al.*, 1990; *Egorov et al.*, 1999). This approach allows for the design of fast algorithms for modeling wave propagation in the atmosphere. The asymptotic algorithm uses the geometric optical solution for bending angles which is transformed by an FIO into the time-dependent wave optical solution. (*Gorbunov*, 2003; *Gorbunov and Lauritsen*, 2004) derived explicit formulas for the operator and constructed an approximation that allows to reduce the operator to a composition of nonlinear coordinate transforms, multiplication with reference signals, and Fourier transforms. The approximation utilizes a canonical transform linearized in the vicinity of a smooth model of the ray manifold. For modeling of multi-channels measurements, it is sufficient to compute the geometric optical solution only once. Since the most time-consuming part of the algorithm is the geometric optical solution, the total computational time only indicates a weak dependence from the number of the channels. On

the contrary, in the phase screen method the computational time is proportional to the number of channels. *Gorbunov* (2003); *Gorbunov and Lauritsen* (2004) also suggested a simple modification of this forward modeling technique based on the inverse Full-Spectrum Inversion (FSI) which has been utilized by *Beyerle et al.* (2006); *Lohmann et al.* (2006).

In modeling wave propagation in a turbulent atmosphere (*Gorbunov and Kirchengast*, 2005) the asymptotic solution cannot be utilized because it does not account for the diffraction on small-scale inhomogeneities inside the atmosphere (the asymptotic forward modelling only accounts for the diffraction due to a large propagation distance). In this case, it is necessary to use the phase screen simulation technique. The final step of this simulation algorithm is the propagation of the waves from the last phase screen to the orbit of the satellite carrying the space-born receiver. In previous versions of the algorithm this step was implemented by the computation of multiple diffractive integrals. This procedure, however, proves to be very slow, especially when computing the propagation of waves with frequencies 9 GHz and higher.

In this paper, we start from the standard solution of the vacuum propagation in the form of the Zverev Transform, which belongs to the class of Fourier Integral Operators (FIO), and construct an approximation that reduces the operator to a composition of a nonlinear coordinate transform, the multiplication with reference signals, and the Fourier transform. To this end, we employ the method based on the linearization of the canonical transform describing the propagation of geometric optical rays (*Gorbunov and Lauritsen*, 2004).

3.2 Fourier Integral Operator Solution for Wave Propagation from the Last Phase Screen to the Observation Orbit

In problems where the account of the small-scale structures of the refractivity field is necessary we cannot use the asymptotic solution (*Gorbunov*, 2003; *Gorbunov and Lauritsen*, 2004). This is due to the fact that this solution only takes into account the diffraction effects due to the large propagation distances, while the diffraction on small-scale inhomogeneities inside the atmosphere is neglected. In such problems it is necessary to model the wave propagation using, for example, the multiple phase screens method. The geometry of wave propagation in the multiple phase screens method is shown in Figure 5. The wave propagation from one screen to the next screen is computed by the standard algorithm utilizing the fast Fourier transform (*Martin*,

1992). The last step of the forward modeling is the propagation of the wave from the last phase screen to the LEO (Low Earth Orbiter) orbit. Because the LEO orbit is a curved line, it is impossible to write the exact solution as a composition of Fourier transforms. Usually, this computation is implemented as a multiple evaluation of the Fresnel diffractive integrals resulting in significant computational costs. Here we apply the FIO technique along with the method based on the linearized canonical transform for constructing a fast algorithm for the propagation of waves from the last phase screen to the LEO orbit.

Consider the computation of the wave field $u(t)$ on the LEO orbit in the vertical plane $(X(t), Z(t))$ with the boundary condition $u_0(z)$ on the last phase screen directed along the vertical axis z at $x = 0$ (Fig. 5). We write the boundary condition in the form $u_0(z) = A(z)\exp(ik\Psi(z))$, assuming that the field equals either a fast-oscillation function with a smooth amplitude or a superposition of such functions.

Next, we derive the FIO that describes the propagation from a straight line to a generic curve. Consider the plane wave (Fourier) expansion:

$$\tilde{u}_0(\eta) = \sqrt{\frac{-ik}{2\pi}} \int u_0(z) \exp\left(-ikz\eta\right) dz. \tag{52}$$

The plane wave with the spatial frequency, or momentum, η has the unit direction vector $\left(\sqrt{1-\eta^2}, \eta\right)$ and, therefore, it has the following form (*Zverev*, 1975):

$$U(x, z, \eta) = \sqrt{\frac{ik}{2\pi}} \tilde{u}_0(\eta) \exp\left(ikx\sqrt{1-\eta^2} + ikz\eta\right). \tag{53}$$

The field $u(t)$ along the curve $(X(t), Z(t))$ equals the sum of all the plane waves and subsequently reads (*Zverev*, 1975):

$$u(t) = \sqrt{\frac{ik}{2\pi}} \int \exp\left[ik\left(X(t)\sqrt{1-\eta^2} + Z(t)\eta\right)\right] \tilde{u}_0(\eta) d\eta. \tag{54}$$

This form of the solution (Zverev Transform) is a FIO of the first kind describing the propagation from a vertical line to a curve. By substituting the Fourier expansion (52) into (54), exchanging the integration order and integrating over η, we can derive the field in the form of the diffractive integral (*Gorbunov and Gurvich*, 1998a,b; *Vladimirov*, 1971):

$$u(t) = \sqrt{\frac{ik}{2\pi}} \int u_0(z) \cos\varphi\left(z, t\right) \frac{\exp\left(ikr\left(z, t\right)\right)}{\sqrt{r\left(z, t\right)}} dz. \tag{55}$$

Here, $r(z,t) = \left((Z(t)-z)^2 + X(t)^2\right)^{1/2}$ is the distance between the observation point $(X(t), Z(t))$ and source point $(0, z)$, and $\varphi(z,t)$ is the angle between the (horizontal) normal vector to the source line and the vector $(X(t), Z(t)-z)$; thus, it follows that $\cos\varphi(z,t) = X(t)/r(z,t)$.

If the field is observed on a vertical line, $X(t) = X = \text{const}$, it is convenient to consider the field as a function of the vertical coordinate Z. In this case, the operator (54) is a composition of a Fourier transform $F_{z\to\eta}$, multiplying with a vacuum propagator in the frequency space $\exp\left(ikX\sqrt{1-\eta^2}\right)$ (i.e., a reference signal), and an inverse Fourier transform $F^{-1}_{\eta\to Z}$. This transform composition is the basis of the multiple phase screens method (*Martin*, 1992).

Below, we construct the approximation that allows, in a similar way, for the computation of the wave propagation from the (last) phase screen to an arbitrary curve. We will rewrite the operator as a composition of the Fourier transform, a nonlinear coordinate transform, the multiplication with a reference signal, the inverse Fourier transform, and one more multiplication with a reference signal. For this purpose we will derive an FIO corresponding to the linearization of the equations for the geometric optical rays in the vicinity of a smooth model of the ray structure. We will use the momentum representation of the field, $\tilde{u}_0(\eta) = A'(\eta)\exp\left(ik\Psi'(\eta)\right)$. The stationary phase point $\eta_s(t)$ of the integral (54) is determined from the following equation:

$$\left(-X(t)\frac{\eta}{\sqrt{1-\eta^2}} + Z(t) + \frac{\partial\Psi'}{\partial\eta}\right)\Bigg|_{\eta=\eta_s(t)} = 0. \tag{56}$$

We also define $z_s(\eta)$ as the funtion inverse to $\eta(z) = \dfrac{d\Psi(z)}{dz}$. Given a moment of time t, $\eta_s(t)$ equals the momentum of the ray arriving at point $(X(t), Z(t))$, and the starting point of the ray is $(0, z_s(\eta_s(t)))$. Both dependencies $\eta_s(t)$ and $z_s(\eta)$ can be multi-valued if multipath propagation takes place in the coordinate or momentum representation (*Mishchenko et al.*, 1990). However, we can always limit our analysis to the field components corresponding to separate branches of the ray manifold with single-valued projections to the coordinate or momentum axis, and afterwards we can take the superposition of such field components. Because the derivative of the eikonal $\Psi'(\eta)$ in the momentum representation equals $-z_s(\eta)$, we can write:

$$Z(t) - z_s(\eta_s(t)) = X(t)\frac{\eta_s(t)}{\sqrt{1-\eta_s^2(t)}}. \tag{57}$$

Consider the canonical transform from the coordinate and momentum (z,η) to the new coordinate and momentum (t,σ), where $\sigma = \omega/k$, with

ω being the Doppler frequency. The generating function of this canonical transform equals the phase function of the operator (54):

$$S_1(t,\eta) = X(t)\sqrt{1-\eta^2} + Z(t)\eta. \tag{58}$$

This function satisfies the following differential equation (*Gorbunov and Lauritsen*, 2004):

$$dS_1 = \sigma dt + z d\eta. \tag{59}$$

This allows for the derivation of the following expressions:

$$\sigma = \frac{\partial S_1}{\partial t} = \dot{X}(t)\sqrt{1-\eta^2} + \dot{Z}(t)\eta, \tag{60}$$

$$z = \frac{\partial S_1}{\partial \eta} = Z(t) - X(t)\frac{\eta}{\sqrt{1-\eta^2}}. \tag{61}$$

For the amplitude function we have the following expression (*Gorbunov and Lauritsen*, 2004):

$$a(t,\eta) = \sqrt{\mu \frac{\partial^2 S_1}{\partial t\, \partial \eta}} = \left(\dot{Z}(t) - \dot{X}(t)\frac{\eta}{\sqrt{1-\eta^2}}\right)^{1/2} \mu^{1/2}, \tag{62}$$

where μ is the measure density defined so as to match energy conservation (*Gorbunov and Lauritsen*, 2004):

$$\left|\tilde{u}_0(\eta)\right|^2 d\eta = \left|u(t)\right|^2 \mu(t,\eta)^{-1} dt. \tag{63}$$

It follows from (54) that $a(t,\eta) = 1$, thus we obtain

$$\mu(t,\eta) = \left(\dot{Z}(t) - \dot{X}(t)\frac{\eta}{\sqrt{1-\eta^2}}\right)^{-1}. \tag{64}$$

Every ray has a starting point z, momentum η, and observation time t. So the ray structure can be parameterically represented as $[z,\eta,t]$, which means that all these varables are looked at as functions of the index j enumerating rays. The corresponding funtions $z(\eta)$ and $t(\eta)$ may be multi-valued (Figure 6).

We shall now obtain a smooth model of the ray structure: $[z_0,\eta_0,t_0]$. Consider the phase of the integrand of the diffractive integral (55): $\Phi(z,t) = \Psi(z) + r(z,t)$. For each moment of time t we find $\bar{z}(t)$ minimizing $\Phi(z,t)$. We compute $\bar{\sigma}(t)$ as the filtered derivative $d\Phi(\bar{z}(t),t)/dt$. Solving (60) for η, we obtain the model $\eta_0(t)$:

$$\eta_0(t) = \frac{\dot{Z}(t)\bar{\sigma}(t) - \operatorname{sign}\left(\dot{Z}(t)\right)\dot{X}(t)\sqrt{\dot{X}^2(t) + \dot{Z}^2(t) - \bar{\sigma}^2(t)}}{\dot{X}^2(t) + \dot{Z}^2(t)}. \tag{65}$$

In addition, the function $\eta_0(t)$ is monotonized so that we can obtain an inverse single-valued function $t_0(\eta)$ and define $z_0(\eta)$ and $\sigma_0(t)$ using (61) and (60):

$$z_0(\eta) = Z(t_0(\eta)) - X(t_0(\eta))\frac{\eta}{\sqrt{1-\eta^2}}, \tag{66}$$

$$\sigma_0(t) = \dot{X}(t)\sqrt{1-\eta_0(t)^2} + \dot{Z}(t)\eta_0(t), \tag{67}$$

Consider the canonical transform $(z,\eta) \to (t,\sigma)$ linearized in the vicinity of the model $z_0(\eta)$:

$$t = t(z,\eta) = t(z_0(\eta),\eta) + \frac{\partial t_0}{\partial z}(z - z_0(\eta)) = t_0(\eta) - \frac{\partial t_0}{\partial z}z_0(\eta) + \frac{\partial t_0}{\partial z}z \equiv f(\eta) + z', \tag{68}$$

where we introduced the ancillary function $f(\eta) \equiv t_0(\eta) - \dfrac{\partial t_0}{\partial z}z_0(\eta)$ and coordinate z', and $\dfrac{\partial t_0}{\partial z}$ denotes the derivative $\dfrac{\partial t(z,\eta)}{\partial z}$ taken at the point $(z_0(\eta),\eta)$.

It is convenient to represent the canonical transform $(z,\eta) \to (t,\sigma)$ as a composition of two canonical transforms, $(z,\eta) \to (z',\xi) \to (t,\sigma)$, where the first step fulfills $z'd\xi = zd\eta$:

$$z' = \frac{\partial t_0}{\partial z}z, \tag{69}$$

$$d\xi = \left(\frac{\partial t_0}{\partial z}\right)^{-1} d\eta. \tag{70}$$

For the generating function $\bar{S}_1(t,\xi)$ of the second step we have the following equation:

$$d\bar{S}_1 = \sigma dt + z'd\xi = \sigma dt + (t - f(\xi))d\xi, \tag{71}$$

where we use the short-form notation $f(\xi)$ instead of $f(\eta(\xi))$. We furthermore complement the canonical transform with the following expansion:

$$\sigma = \sigma(t,\eta) = \sigma(t,\eta_0(t)) + \frac{\partial \sigma_0}{\partial \eta}(\eta - \eta_0(t)). \tag{72}$$

Now, dS_1 is a full differential, therefore: $\left(\dfrac{\partial \sigma}{\partial \eta}\right)_t = \left(\dfrac{\partial z}{\partial t}\right)_\eta$. Utilizing the definition of ξ, we arrive at the following relationship:

$$\frac{\partial \sigma_0}{\partial \eta}(\eta - \eta_0(t)) = \left(\frac{\partial t_0}{\partial z}\right)^{-1}(\eta - \eta_0(t)) = \xi - \xi_0(t), \tag{73}$$

with $\xi_0(t) = \xi(\eta_0(t))$. From this it follows that

$$\sigma = \sigma(t,\eta) = \sigma_0(t) - \xi_0(t) + \xi \equiv g(t) + \xi, \tag{74}$$

where we introduced the second ancillary function $g(t) = \sigma_0(t) - \xi_0(t)$.

Therefore, we have the following equation for the generating function:

$$\begin{aligned} d\bar{S}_1 &= (g(t)+\xi)dt + (t - f(\xi))d\xi, & (75)\\ \bar{S}_1(t,\xi) &= \int g(t)dt - \int f(\xi)d\xi + t\xi. & (76) \end{aligned}$$

The derivative $\dfrac{\partial t_0}{\partial z}$ is evaluated as follows:

$$\begin{aligned} \frac{\partial t_0}{\partial z} &= \left.\frac{\partial t(z,\eta)}{\partial z}\right|_{z=z_0(\eta)} = \left.\left(\frac{\partial z(t,\eta)}{\partial t}\right)^{-1}\right|_{t=t_0(\eta)} = \\ &= \left.\left(\frac{\partial^2 S_1(t,\eta)}{\partial\eta\partial t}\right)^{-1}\right|_{t=t_0(\eta)} = \left.\left(\dot{Z}(t) - \dot{X}(t)\frac{\eta}{\sqrt{1-\eta^2}}\right)^{-1}\right|_{t=t_0(\eta)}. \end{aligned} \tag{77}$$

This allows for the derivation of the following expression for the ancillary function $f(\eta)$:

$$f(\eta) = t_0(\eta) - \frac{\partial t_0}{\partial z} z_0(\eta) = t_0(\eta) - \frac{Z(t_0(\eta))\sqrt{1-\eta^2} - X(t_0(\eta))\eta}{\dot{Z}(t_0(\eta))\sqrt{1-\eta^2} - \dot{X}(t_0(\eta))\eta}. \tag{78}$$

In addition, the momentum ξ has the form:

$$\xi(\eta) = \int_0^\eta \left(\dot{Z}(t_0(\eta')) - \dot{X}(t_0(\eta'))\frac{\eta'}{\sqrt{1-\eta'^2}}\right) d\eta'. \tag{79}$$

The second ancillary function $g(t)$ is evaluated as follows:

$$g(t) = \sigma_0(t) - \xi_0(t) = \dot{X}(t)\sqrt{1-\eta_0^2(t)} + \dot{Z}(t)\eta_0(t) - \xi(\eta_0(t)). \tag{80}$$

Instead of $\mu(t,\eta)$ we introduce the measure density ν in the coordinates (t,ξ): $\nu(t,\xi)$. Introducing the short-form notation $\tilde{u}_0(\xi) = \tilde{u}_0(\eta(\xi))$ and using the following definition of the measure density:

$$|\tilde{u}_0(\xi)|^2 d\xi = |u(t)|^2 \nu(t,\xi)^{-1} dt, \tag{81}$$

we obtain the relationship:

$$|\tilde{u}_0(\xi)|^2 d\xi \frac{d\eta}{d\xi} = |u(t)|^2 \nu(t,\xi)^{-1} \frac{d\eta}{d\xi} dt = |u(t)|^2 \mu(t,\eta)^{-1} dt. \tag{82}$$

From this we derive the expression for the measure density:

$$\begin{aligned} \nu(t,\xi)^{-1} = \mu(t,\eta)^{-1} \frac{d\xi}{d\eta} = \\ = \left(\dot{Z}(t) - \dot{X}(t) \frac{\eta}{\sqrt{1-\eta^2}} \right) \left(\dot{Z}(t_0(\eta)) - \dot{X}(t_0(\eta)) \frac{\eta}{\sqrt{1-\eta^2}} \right) \approx \\ \approx \left(\dot{Z}(t_0(\eta)) - \dot{X}(t_0(\eta)) \frac{\eta}{\sqrt{1-\eta^2}} \right)^2. \end{aligned} \tag{83}$$

Finally, we arrive at the following expression for the desired FIO in (54):

$$u(t) = \sqrt{\frac{ik}{2\pi}} \exp\left(ik \int g(t) dt \right) \int \sqrt{\nu\left(t_0(\xi), \xi\right)} \exp\left(ikt\xi\right) \exp\left(-ik \int f(\xi) d\xi \right) \tilde{u}_0(\eta(\xi)) d\xi, \tag{84}$$

which can be written as

$$u(t) = \sqrt{\frac{ik}{2\pi}} \exp\left(ik \int g(t) dt \right) \int \exp\left(ikt\xi\right) \frac{\exp\left(-ik \int f(\xi) d\xi\right) \tilde{u}_0(\eta(\xi))}{\dot{Z}(t_0(\xi)) - \dot{X}(t_0(\xi)) \dfrac{\eta(\xi)}{\sqrt{1-\eta(\xi)^2}}} d\xi. \tag{85}$$

Thus, we have obtained the FIO solution for the propagation of the field from a vertical line (the last phase screen) to the observation curve. This operator is an approximate form of the exact Zverev Transform (54), where for the derivation of the phase function we used the geometric optical ray equations linearized in the vicinity of a smooth model solution. This linearization allows representing the Zverev Transform (54) as a combination of the Fourier transform and multiplication with reference signals, and therefore it allows for an effective numerical implementation as an FFT.

3.3 Numerical Simulations

In order to test the accuracy and performance of the FIO-based methods of computation of wave propagation in the atmosphere, we carried out a series of numerical simulations. For modeling the atmospheric refractivity we used global gridded fields of meteorological parameters from the re-analysis of European Center for Medium-Range Weather Forecasts (ECMWF). We

consider the problem with the stationary transmitter. In order to reduce the geometry with the moving GPS satellite to a geometry with a stationary transmitter, the coordinate transform from (*Gorbunov*, 2002a) is used. The field on the first phase screen equals the spherical wave from the transmitter in a vacuum. We compare the following three methods of the computation of wave propagation as illustrated by Figure 5.

1. Multiple phase screens and the propagation from the last phase screen to the LEO orbit by diffractive integrals (MPS-DI).

2. Multiple phase screens and the propagation from the last phase screen by the Linearized Zverev Transform (LZT) described in (85) (MPS-LZT).

3. Asymptotic forward modeling technique using FIO (AFM) as described in (*Gorbunov and Lauritsen*, 2004) (where abbreviation AS was used).

Figure 7 shows the amplitude of the simulated observed radio signal as a function of time. The typical duration of an RO measurement is 1–1.5 minutes. For the frequency 1.5 GHz (one of the GPS channels) the sampling rate of the measurement is 50 Hz. Therefore, in each RO event 3000 – 5000 samples in each frequency channel are measured. The amplitude on the observation curve is a very convenient quantity for the comparison of different methods of numerical wave propagation, because it is very sensitive to any phase perturbations. In the single-path propagation area before 69 s, all the three methods give very similar results. After 69 s the multipath area begins. Here the second method of propagation from the last phase screen yields results very close to the accurate 1st method based on the diffractive integrals. The accuracy of the 3rd method is slightly worse, although it also reproduces the structure of the amplitude well. Here, the computational time (on a system with a Pentium 4 processor, 3.00 GHz) is 9 min for the 1st method (MPS-DI), it is about 3 min for both the 2nd and 3rd methods (MPS-LZT and AFM, respectively).

Figure 8 shows the results for the same atmospheric state and observation geometry, but for a frequency of 9.6 GHz. In this case the sampling rate should be not less than 1000 Hz. Therefore, the number of samples in this frequency channel can reach a value of 100000. For the first method (MPS-DI), this results in many hours of numerical computations (7 hours on a system with a Pentium 4 processor, 3.00 GHz). The numerical computation based on the 2nd method (MPS-LZT) is much more effective and requires 10 minutes on the same system, simultaneously providing a high accuracy. The 3rd, asymptotic method (AFM) has the highest performance and requires as little as 3 minutes; however, its accuracy is slightly worse.

3.4 Conclusions

We discussed the application of the FIO technique for modeling wave propagation in the atmosphere. Asymptotic solutions of wave problems based on Maslov operators or FIO (these two techniques are equivalent) are well-known and widely used. However, they cannot be applied for modeling the effects of diffraction on small-scale atmospheric inhomogeneities. In this case it is necessary to use the multiple phase screens approach. The screen-to-screen propagation allows for an effective numerical implementation based on FFT. However, the last step, propagation from the last phase screen to the curved LEO orbit was previously implemented by the computation of multiple Fresnel integrals. In this paper we focused on constructing a method for the vacuum propagation from the last phase screen to the observation curve that allows for an effective numerical implementation. The exact Zverev Transform solution of this problem can be written in the form of an FIO. The phase function of the FIO is the generating function of the canonical transform describing the propagation of straight rays in a vacuum. The basic idea of our work consists of the approximation of using the linearization of the canonical transform in the vicinity of a smooth model of the ray manifold. This reduces the FIO to a composition of nonlinear coordinate transforms, multiplications with reference signals, and the Fourier transform. Each of these steps allows for an effective numerical implementation.

We performed a numerical comparison of three methods of the computation of the field of radio waves diffracted by the atmosphere: 1) the wave propagation in the atmosphere by the multiple phase screen method, and the propagation from the last phase screen to the LEO orbit by multiple diffractive (Fresnel) integrals; 2) the wave propagation in the atmosphere by the multiple phase screen method, and the propagation from the last phase screen to the LEO orbit in the form of an FIO, and 3) a full asymptotic solution of the forward modelling of the wave problem. Our results show that the vacuum propagation to the LEO orbit by the FIO has a much better performance compared to the computation of multiple diffractive integrals. High accuracy and numerical efficiency of the method is confirmed by numerical simulations based on realistic gridded fields of meteorological parameters.

We have derived the linearized Zverev Transform that solves the problem of the wave propagation from a straight line to a curve. It is straightforward to invert this operator and thereby obtain a fast solution of the propagation from a generic curve to a straight line. As a result, this allows for a linearized, fast implementation of the Back Propagation (BP) formerly used for RO data processing. It is also possible to combine the propagation from a source curve to an intermediate straight line with the successive propagation from

the intermediate straight line to an observation curve. This allows for the design of fast algorithms for the propagation of waves between two generic curves.

4 Turbulent random refractivity field modeling

We used a model of the turbulent atmosphere, which includes a regular background part from European Centre for Medium-Range Weather Forecast (ECMWF) ERA40 re-analyses complemented with anisotropic turbulence with a magnitude chosen as estimated from high-resolution (∼10 m vertical spacing) radio sonde measurements. The re-analysis fields were given on a latitudinal-longitudinal grid with $0.5^\circ \times 0.5^\circ$ resolution and on 64 vertical levels up to a height of about 60 km. Turbulence was modeled as a random relative perturbation of the refractivity field with a power form of the spectrum:

$$\tilde{B}(\kappa) = \begin{cases} \tilde{c}\kappa_{ext}^{-\mu}, \ \kappa < \kappa_{ext} \\ \tilde{c}\kappa^{-\mu}, \ \kappa_{ext} \le \kappa \le \kappa_{int} \\ \tilde{c}\kappa^{-\mu} \exp\left[-\left(\dfrac{\kappa - \kappa_{int}}{\kappa_{int}/4} \right)^2 \right], \ \kappa > \kappa_{int} \end{cases}, \tag{86}$$

where $\kappa = \left(\kappa_z^2 + q^2 \dfrac{\kappa_\theta^2}{r_E^2} \right)^{1/2}$, κ_z and κ_θ are the spatial frequencies (wave numbers) conjugated to the polar coordinates z and θ in the occultation plane (z being the height above the Earth's surface, θ being the polar angle), r_E is the Earth's curvature radius, q is the anisotropy coefficient ($q > 1$, horizontally stretched turbulence). Factor $\tilde{c}$ normalizes the rms turbulent fluctuations to unity. In the coordinate space we use an additional factor $c(z)$, which describes the relative magnitude of turbulent perturbations as a function of altitude. We assumed that the radiosonde-derived fractional refractive index variations are primarily due to turbulence, and we did not model the intermittence of the turbulence. These assumptions can result in an overestimate of the turbulence fluctuation intensity. However, this will be favorable for a conservative (upper-bound oriented) assessment of the method in terms of which transmission retrieval error levels are to be expected.

Our model is based on the theoretical and experimental studies (*Fritts et al.*, 1988; *Fritts and VanZandt*, 1993; *Fritts and Alexander*, 2003; *Gurvich and Brekhovskikh*, 2001; *Gurvich and Chunchuzov*, 2003, 2005). *Gurvich and Chunchuzov* (2003, 2005) revealed that atmospheric turbulence is a mixture of isotropic (Kolmogorov) component and strongly anisotropic component, which has properties similar to internal gravity waves. We adopted the turbulence to be characterized by an external scale $2\pi/\kappa_{ext} = 100$ m, internal scale $2\pi/\kappa_{int} = 15$ m, exponent $\mu = -4$ for the 2D spectrum (corresponding to exponent $\mu_{3D} = -5$ for the 3D spectrum) that follows (*Gurvich and*

Chunchuzov, 2003, 2005). (*Yakovlev et al.*, 2003) obtained a close value of $\mu_{3D} = 4.5$.

The value of 100 m for the outer scale of turbulence has been chosen consistent with a parameterized turbulence modeling in previous ACE+ LEO-LEO studies (*Kirchengast et al.*, 2004b,a; *Kirchengast and Høeg*, 2004). It is a realistic estimate for altitudes 5 to 15 km based on observations of turbulence parameters reported, for example, by *Eaton and Nastrom* (1998); *Rao et al.* (2001) The outer scale typically lies around 50 - 150 m. The internal scale is chosen close to the diffractive limit (*Gorbunov et al.*, 2004): $h \geq \sqrt[3]{2\lambda^2 r_E}$, which is about 20 m. Input of smaller scales into the amplitude scintillation will be very small due to both the decrease of spectral density of turbulence and diffraction. According to experimental studies (*Kan et al.*, 2002; *Yakovlev et al.*, 1995, 2003), the maximum input into the amplitude fluctuations comes from scales of about 100 m. According to (*Gurvich and Chunchuzov*, 2003, 2005), amplitude fluctuation intensity increases as a function of anisotropy coefficient q until q reaches a value of about 30, where the increase practically saturates. We simulated q equal to 3, 5, 10, 20, and 50, which covers all the characteristic range of q. Our turbulence model results in a realistic pattern of scintillations of the simulated signals looking similar to the experimentally observed ones (*Kan et al.*, 2002; *Yakovlev et al.*, 1995, 2003).

For generating realizations of the field $f(z, \theta)$ of relative perturbation of refractivity, we proceed as follows. We specify a coordinate box $(z, \theta) \in [0, Z] \times [0, \Theta]$, where parameters Z and Θ are the vertical and horizontal sizes of the box. Random field $f(z, \theta)$ is generated inside the box and periodically extrapolated outside it. For the high-resolution simulations we choose $Z =$ 4 km and $\Theta = 0.02$ rad. This scheme allows for the reduction of the number of discrete points for the gridded random field down to a number that can be handled by computational system (not exceeding $2^{22} = 4194304$). The discretization steps were chosen in order to resolve the smallest perturbation scales and to adjust the number of grid points to the right-nearest power of 2:

$$\Delta z = Z \cdot 2^{-\text{Ceiling}\ \log_2\ 4\frac{Z}{\Delta z_{\text{int}}}},$$

$$\Delta\theta = \Theta \cdot 2^{-\text{Ceiling}\ \log_2\ 4\frac{\Theta r_E}{q\Delta z}},$$

where Ceiling is the function equal to the right-nearest integer. This allows for forming grids in the coordinate and frequency spaces:

$$
\begin{array}{rl}
z_i = i\Delta z, & i = 0..N_Z - 1 \\
\theta_j = j\Delta\theta, & j = 0..N_\Theta - 1 \\
\kappa_{z,i} = i\dfrac{2\pi}{Z}, & i = -\dfrac{N_Z}{2} + 1, \dfrac{N_Z}{2} \\
\kappa_{\theta,j} = i\dfrac{2\pi}{\Theta}, & j = -\dfrac{N_\Theta}{2} + 1, \dfrac{N_\Theta}{2}
\end{array}
$$

The Fourier transform of a random realization of the statistically homogeneous field $f_{ij} = f\left(z_i, \theta_j\right)$ equals

$$
\tilde{f}_{ij} = \sqrt{\tilde{B}\left(\left(\kappa_{z,i}^2 + q^2 \frac{\kappa_{\theta,j}^2}{r_E^2}\right)^{1/2}\right)} \exp\left(i\varphi_{ij}\right),
$$

where φ_{ij} are random non-correlated phases with a homogeneous distribution inside the interval of $[0, 2\pi]$. The realization of the random field is obtained as follows:

$$
f_{ij} = c(z_i) F^{-1}\left[\tilde{f}_{ij}\right],
$$

where F^{-1} is the inverse Fourier transform, and the factor of $c(z)$ describes the relative magnitude of turbulent perturbations as a function of altitude.

Acknowledgement 1 *The authors acknowledge valuable discussions related to this work with A. S. Gurvich (Institute for Atmospheric Physics, Moscow, Russia) and A. S. Jensen (Danish Met Institute, Copenhagen, Denmark). J. Fritzer (Wegener Center, Univ. of Graz, Austria) is thanked for collaboration and support in implementing the wave-optics forward modeling and retrieval algorithms described into the EGOPS software system. The work was supported by the Russian Foundation for Basic Research and a major part of the work was funded by the ESA Prodex Arrangement No. 90152-CN1 (Project Advanced Topics in RO Modelling and Retrieval).*

5 References

References

Arnold, V. I., *Mathematical Methods of Classical Mechanics*, Springer-Verlag, New York, 1978.

Beyerle, G., T. Schmidt, J. Wickert, S. Heise, M. Rothacher, G. König-Langlo, and K. B. Lauritsen, Observations and simulations of receiver-induced refractivity biases in GPS radio occultation, *J. Geophys. Res.*, *111*, D12101, doi:10.1029/2005JD006673, 2006.

Born, M., and E. Wolf, *Principles of Optics. Vol*, Pergamon Press, New York, 1964.

Eaton, F. D., and G. D. Nastrom, Preliminary estimates of the vertical profiles of inner and outer scales from white sands missile range, new mexico, VHF radar observations, *Radio Science*, *33*, 895 (98RS01,254), 1998.

Egorov, Y. V., *Lectures on Partial Differential Equations. Additional Chapters*, Moscow State University Press, Moscow, 1985, (In Russian).

Egorov, Y. V., A. I. Komech, and M. A. Shubin, *Elements of the Modern Theory of Partial Differential Equations*, Springer-Verlag, Berlin, 1999.

Eshleman, V. R., D. O. Muhleman, P. D. Nicholson, and P. G. Steffes, Comment on absorbing regions in the atmosphere of Venus as measured by radio occultation, *Icarus*, *44*, 793–803, 1980.

Fritts, D. C., and M. J. Alexander, Gravity waves dynamics and effects in the middle atmosphere, *Reviews of Geophysics*, *41*, 1/1003, doi:10.1029/2001RG000,106, 2003.

Fritts, D. C., and T. E. VanZandt, Spectral estimates of gravity wave energy and momentum fluxes. part 1: Energy dissipation, acceleration, and constrains, *Journal of the Atmospheric Sciences*, *50*, 3685–3694, 1993.

Fritts, D. C., T. Tsuda, T. Sato, S. Fukao, and S. Kato, Observational evidence of a saturated gravity wave spectrum in the troposphere and lower stratosphere, *J. Atmos. Sci.*, *45*, 1741 1758, 1988.

Gorbunov, M. E., Canonical transform method for processing GPS radio occultation data in lower troposphere, *Radio Sci.*, *37*, 9–1–9–10, doi:10.1029/2000RS002,592, 2002a.

Gorbunov, M. E., Radio-holographic analysis of Microlab-1 radio occultation data in the lower troposphere, *J. Geophys. Res. - Atm.*, *107*, 7–1–7–10, doi: 10.1029/2001JD000,889, 2002b.

Gorbunov, M. E., An asymptotic method of modeling radio occultations, *J. Atm. Sol.-Terrestr. Phys.*, *65*, 1361–1367, 2003.

Gorbunov, M. E., and A. S. Gurvich, Microlab-1 experiment: Multipath effects in the lower troposphere, *Journal of Geophysical Research*, *103*, 13,819–13,826, 1998a.

Gorbunov, M. E., and A. S. Gurvich, Algorithms of inversion of Microlab-1 satellite data including effects of multipath propagation, *International Journal of Remote Sensing*, *19*, 2283–2300, 1998b.

Gorbunov, M. E., and G. Kirchengast, Processing X/K band radio occultation data in the presence of turbulence, *Radio Science*, *40*, RS6001, doi: 10.1029/2005RS003,263, 2005.

Gorbunov, M. E., and K. B. Lauritsen, Canonical transform methods for radio occultation data, *Scientific Report 02-10*, Danish Meteorological Institute, Copenhagen, Denmark, 2002, http://www.dmi.dk/dmi/Sr02-10.pdf.

Gorbunov, M. E., and K. B. Lauritsen, Analysis of wave fields by Fourier Integral Operators and its application for radio occultations, *Radio Sci.*, *39*, RS4010, doi:10.1029/2003RS002,971, 2004.

Gorbunov, M. E., H.-H. Benzon, A. S. Jensen, M. S. Lohmann, and A. S. Nielsen, Comparative analysis of radio occultation processing approaches based on Fourier integral operators, *Radio Sci.*, *39*, RS6004, doi:10.1029/2003RS002,916, 2004.

Gurvich, A. S., and V. L. Brekhovskikh, Study of the turbulence and inner waves in the stratosphere based on the observations of stellar scintillations from space: A model of scintillation spectra, *Waves in Random Media*, *11*, 163–181, 2001.

Gurvich, A. S., and I. P. Chunchuzov, Parameters of the fine density structure in the stratosphere obtained from spacecraft observations of stellar scintillations, *J. Geophys. Res.*, *108*, 4166, doi:10.1029/2002JD002,281, 2003.

Gurvich, A. S., and I. P. Chunchuzov, Estimates of characteristic scales in the spectrum of internal waves in the stratosphere obtained from

space observations of stellar scintillations, *J. Geophys. Res.*, *110*, 3114, doi:10.1029/2004JD005,199, 2005.

Hajj, G. A., E. R. Kursinski, L. J. Romans, W. I. Bertinger, and S. S. Leroy, A technical description of atmospheric sounding by gps occultation, *J. Atm. Solar-Terrestr. Phys.*, *64*, 451–469, 2002.

Hocke, K., A. G. Pavelyev, O. I. Yakovlev, L. Barthes, and N. Jakowski, Radio occultation data analysis by the radioholographic method, *Journal of Atmospheric and Solar-Terrestrial Physics*, *61*, 1169–1177, 1999.

Hörmander, L., *The Analysis of Linear Partial Differential Operators*, vol. III. Pseudo-Differential Operators, Springer-Verlag, New York, 1985a.

Hörmander, L., *The Analysis of Linear Partial Differential Operators*, vol. IV. Fourier Integral Operators, Springer-Verlag, New York, 1985b.

Igarashi, K., A. Pavelyev, K. Hocke, D. Pavelyev, I. A. Kucherjavenkov, S. Matyugov, A. Zakharov, and O. Yakovlev, Radio holographic principle for observing natural processes in the atmosphere and retrieving meteorological parameters from radio occultation data, *Earth, Planets, and Space*, *52*, 893–899, 2000.

Jensen, A. S., M. S. Lohmann, H.-H. Benzon, and A. S. Nielsen, Full spectrum inversion of radio occultation signals, *Radio Sci.*, *38*, 6–1–6–15, doi: 10.1029/2002RS002,763, 2003.

Jensen, A. S., M. S. Lohmann, A. S. Nielsen, and H.-H. Benzon, Geometrical optics phase matching of radio occultation signals, *Radio Sci.*, *39*, RS3009, doi: 10.1029/2003RS002,899, 2004.

Kan, V., S. S. Matyugov, and O. I. Yakovlev, The structure of stratospheric irregularities according to radio-occultation data obtained using satellite-to-satellite paths, *Izvestiya VUZov, Radiofizika*, *XLV*, 652–663, 2002.

Kirchengast, G., and P. Høeg, The ACE+ mission: Atmosphere and climate explorer based on GNSS-LEO and LEO-LEO radio occultation, in *Occultations for Probing Atmosphere and Climate*, edited by A. K. S. G. Kirchengast, U. Foelsche, pp. 201–220, Springer, Berlin - Heidelberg, 2004.

Kirchengast, G., J. Fritzer, M. Schwaerz, S. Schweitzer, and L. Kornblueh, The atmosphere and climate explorer mission ACE+: Scientific algorithms and performance overview, *Tech. Report for ESA/ESTEC No. 2/2004*, Inst. for Geophys., Astrophys., and Meteorol., Univ. of Graz, Austria, 2004a.

Kirchengast, G., S. Schweitzer, J. Ramsauer, J. Fritzer, and M. Schwaerz, Atmospheric profiles retrieved from ACE+ LEO-LEO occultation data: Statistical performance analysis using geometric optics processing, *Tech. Report for ESA/ESTEC No. 1/2004*, Inst. for Geophys., Astrophys., and Meteorol., Univ. of Graz, Austria, 2004b.

Kravtsov, Y. A., and Y. I. Orlov, *Geometrical optics of inhomogeneous media*, Springer, Berlin, 1990.

Lindal, G. F., J. R. Lyons, D. N. Sweetnam, V. R. Eshleman, D. P. Hinson, and G. L. Tyler, The atmosphere of Uranus: Results of radio occultation measurements with Voyager, *Journal of Geophysical Research*, *92*, 14,987–15,001, 1987.

Lohmann, M. S., A. S. Jensen, H.-H. Benzon, and A. S. Nielsen, Application of window functions for full spectrum inversion of cross-link radio occultation data, *Radio Sci.*, *41*, RS3001, doi:10.1029/2005RS003273, 2006.

Marouf, E. A., G. L. Tyler, and P. A. Rosen, Profiling Saturn rings by radio occultation, *ICARUS*, *68*, 120–166, 1986.

Martin, J., Simulation of wave propagation in random media: theory and applications, in *Wave propagation in random media (scintillations)*, edited by V. I. Tatarskii, A. Ishimaru, and V. U. Zavorotny, pp. 463–486, SPIE - The International Society for Optical Engineering and Institute of Physics Publishing, Bellingham, Washington USA, Bristol and Philadelphia, 1992.

Maslov, V. P., and M. V. Fedoriuk, *Semi-Classical Approximations in Quantum Mechanics*, D.Reidel Publishing Company, Dordrecht, 1981.

Melbourne, W. G., E. S. Davis, C. B. Duncan, G. A. Hajj, K. R. Hardy, E. R. Kursinski, T. K. Meehan, and L. E. Young, *The Application of Spaceborne GPS to Atmospheric Limb Sounding and Global Change Monitoring*, JPL Publ. 94-18, Jet Propul. Lab., Pasadena Calif., 1994.

Mishchenko, A. S., V. E. Shatalov, and B. Y. Sternin, *Lagrangian manifolds and the Maslov operator*, Springer-Verlag, Berlin - New York, 1990.

Mortensen, M. D., and P. Høeg, Inversion of GPS occultation measurements using Fresnel diffraction theory, *Geophysical Research Letters*, *25*, 2441–2444, 1998.

Mortensen, M. D., R. P. Linfield, and E. R. Kursinski, Vertical resolution approaching 100 m for GPS occultations of the earth's atmosphere, *Radio Sci.*, *36*, 1475–1484, 1999.

Pavelyev, A., K. Igarashi, C. Reigber, K. Hocke, J. Wickert, G. Beyerle, S. Matyugov, A. Kucherjavenkov, D. Pavelyev, and O. Yakovlev, First application of the radioholographic method to wave observations in the upper atmosphere, *Radio Sci.*, *37*, 15–1–15–11, doi: 10.1029/2000RS002,501, 2002.

Pavelyev, A. G., On the feasibility of radioholographic investigations of wave fields near the Earth's radio-shadow zone on the satellite-to-satellite path, *J. of Comm. Techn. and Elec.*, *43*, 875–879, 1998.

Rao, D. N., T. N. Rao, M. Venkataratnam, P. Srinivasulu, and P. B. Rao, Diurnal and seasonal variability of turbulence parameters observed with Indian mesosphere-stratosphere-troposphere radar, *Radio Science*, *36*, 1439 (2000RS002,316), 2001.

Sokolovskiy, S. V., Modeling and inverting radio occultation signals in the moist troposphere, *Radio Sci.*, *36*, 441–458, 2001.

Vladimirov, V. S., *Equations of Mathematical Physics*, Pure and applied mathematics, 3, M. Dekker, New York, 1971, vi, 418 p. illus. 24 cm.

Vorob'ev, V. V., and T. G. Krasil'nikova, Estimation of the accuracy of the atmospheric refractive index recovery from Doppler shift measurements at frequencies used in the NAVSTAR system, *Izvestiya Academy of Sciences SSSR, Atmospheric and Oceanic Physics, English Translation*, *29*, 602–609, 1994.

Yakovlev, O. I., S. S. Matyugov, and I. A. Vilkov, Attenuation and scintillation of radio waves in the Earth's atmosphere from radio occultation experiment on satellite-to-satellite links, *Radio Science*, *30*, 591–602, 1995.

Yakovlev, O. I., S. S. Matyugov, and V. A. Anufriev, Scintillations of centimeter waves and the atmospheric irregularities from radio occultation data, *Radio Sci.*, *38*, doi: 10.1029/2000RS002,546, 2003.

Zverev, V. A., *Radio-optics*, Soviet Radio, Moscow, 1975.

6 Figures

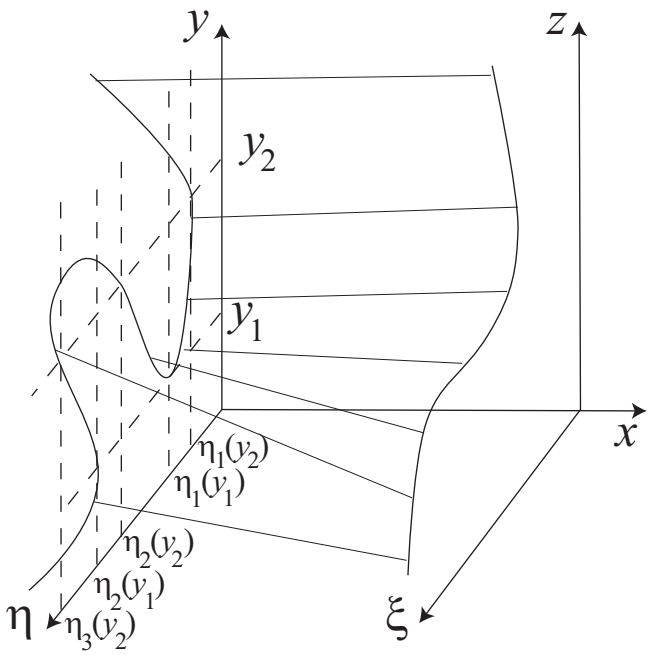

Figure 1: Schematic ray manifold in the phase space with different types of its projection to coordinate axes.

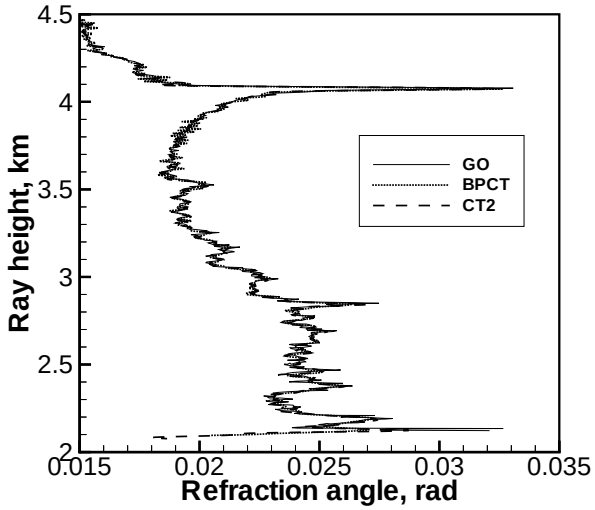

Figure 2: Comparison of different modifications of the CT technique. Refraction angle profiles as functions of ray height (impact parameter minus Earth's curvature radius): (1) reference geometric optical solution (GO, solid line), (2) standard composition of BP and CT (BPCT, dotted line), and (3) CT2 algorithm (dashed line).

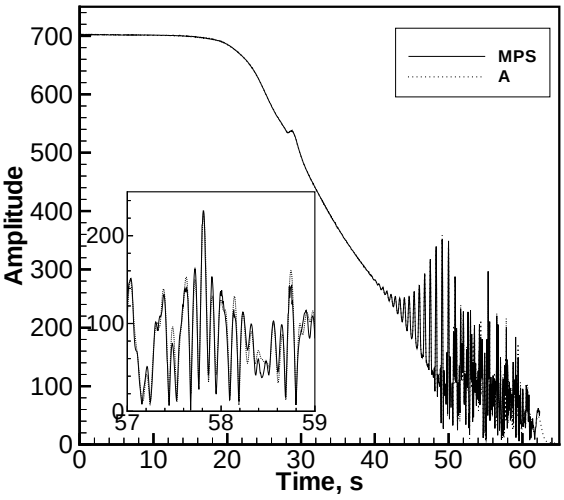

Figure 3: Validation of asymptotic direct modeling. Amplitude of simulated radio occultation signal as function of time: (1) MPS simulation (solid line) and (2) asymptotic simulation based on the FIO2 (A, dotted line).

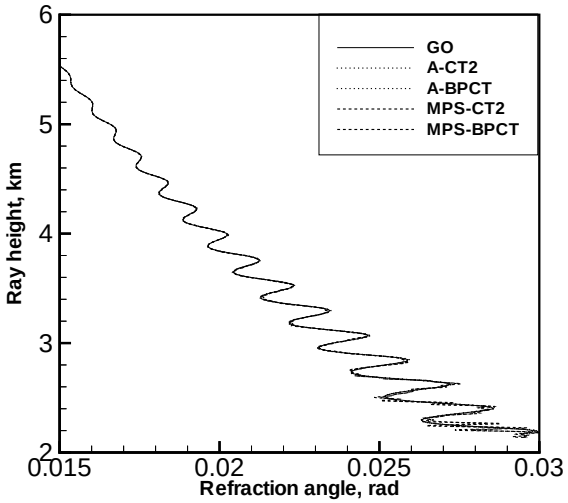

Figure 4: Refraction angle profiles from geometric optical ray tracing and from simulated radio occultation data: (1) reference GO profile (GO, solid line), (2) asymptotic simulation processed by CT2 (A-CT2, dotted line), (3) asymptotic simulation processed by BP+CT (A-BPCT, dotted line), (4) MPS simulation processed by CT2 (MPS-CT2, dashed line), and (5) MPS simulation processed by BP+CT (MPS-BPCT, dashed line).

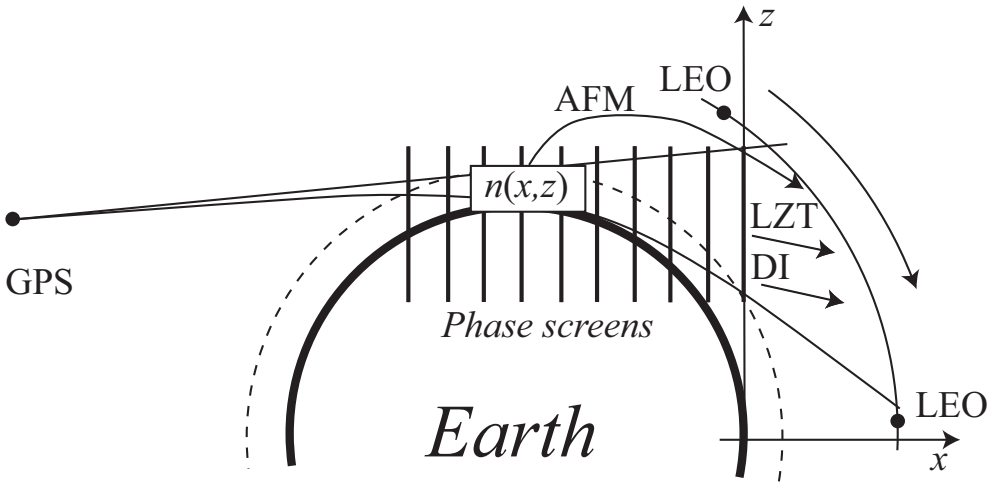

Figure 5: Geometry of the simulation of wave propagation by different techniques. Asymptotic forward modeling (AFM) uses the refractivity field $n(x, z)$ to obtain the geometric optical bending angle solution, which is transformed to the asymptotic time-dependent wave solution. Multiple phase screens (MPS) technique requires the propagation of the field from the last phase screen to the LEO orbit. This can be done by diffractive integrals (DI) or by the Linearized Zverev Transform (LZT).

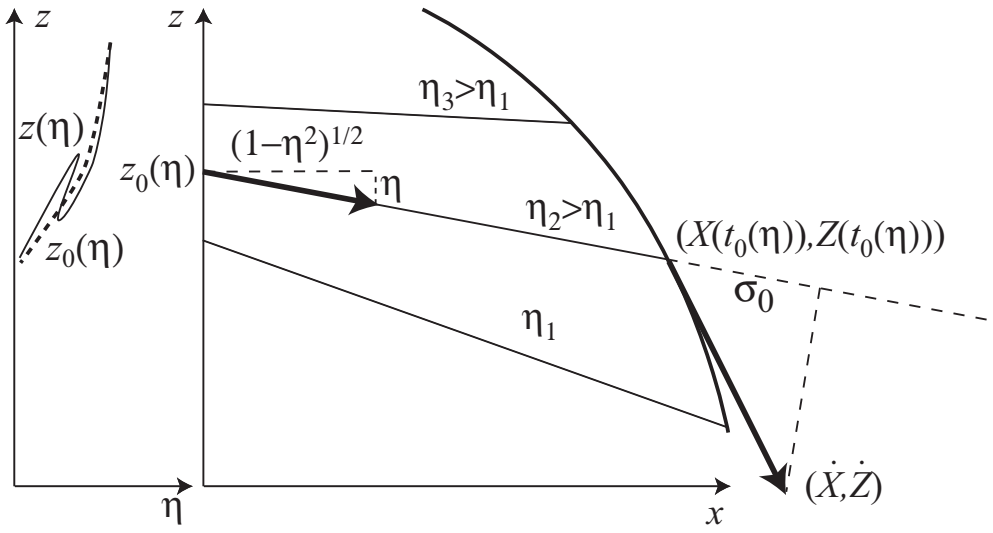

Figure 6: Ray manifold $z(\eta)$ (left panel: solid line) may be a multi-valued function. We define a smooth model $\eta_0\,(t)$ to be a monotonous function. This allows for the definition of smooth models $z_0(\eta)$ (left panel: heavy dashed line) and $t_0\,(\eta)$ with unique projections to the η axis.

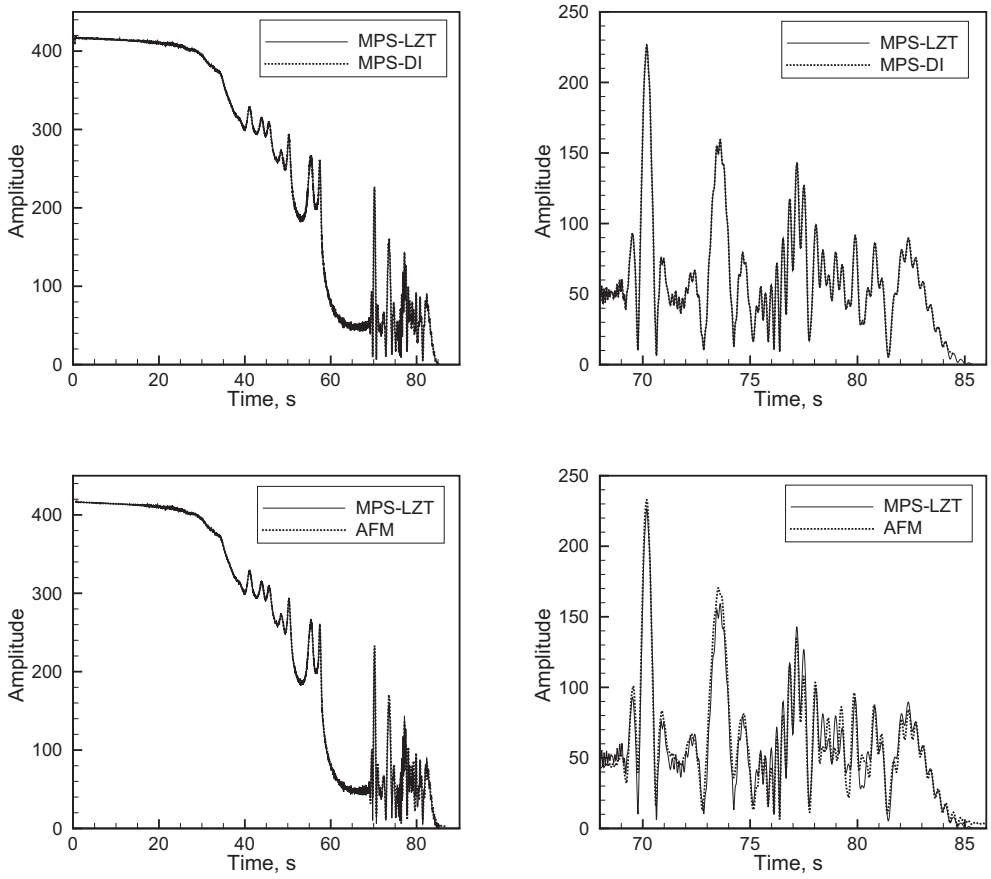

Figure 7: The numerical simulation of the propagation of a signal with a frequency of 1.5 GHz. We compare three methods: 1) multiple phase screens and the propagation from the last phase screen to the LEO orbit by the diffractive integrals (MPS-DI), 2) multiple phase screens and the propagation from the last phase screen by the LZT (MPS-LZT), and 3) asymptotic forward modeling by FIO (AFM).

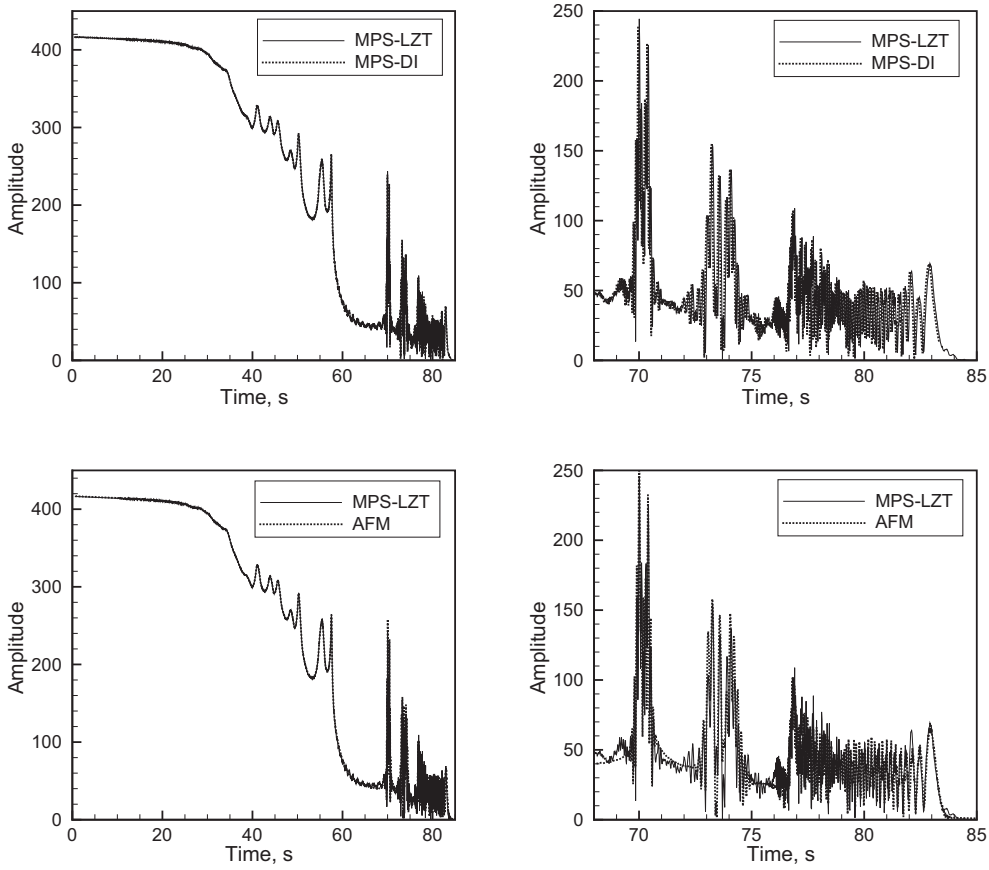

Figure 8: The numerical simulation of the propagation of a signal with a frequency of 9.6 GHz. We compare three methods: 1) multiple phase screens and the propagation from the last phase screen to the LEO orbit by the diffractive integrals (MPS-DI), 2) multiple phase screens and the propagation from the last phase screen by the LZT (MPS-LZT), and 3) asymptotic forward modeling by FIO (AFM).